

## RESEARCH ARTICLE

# Signal inhibitory receptor on leukocytes-1 recognizes bacterial and endogenous amphipathic $\alpha$ -helical peptides

Matevž Rumpret<sup>1,2</sup>  | Helen J. von Richthofen<sup>1,2</sup>  | Maarten van der Linden<sup>1</sup>  | Geertje H. A. Westerlaken<sup>1,2</sup> | Cami Talavera Ormeño<sup>2,3</sup>  | Jos A. G. van Strijp<sup>4</sup>  | Meytal Landau<sup>5</sup>  | Huib Ovaa<sup>2,3†</sup> | Nina M. van Sorge<sup>4</sup>  | Linde Meyaard<sup>1,2</sup> 

<sup>1</sup>Center for Translational Immunology, University Medical Center Utrecht, Utrecht University, Utrecht, The Netherlands

<sup>2</sup>Oncode Institute, Utrecht, The Netherlands

<sup>3</sup>Department of Cell and Chemical Biology, Leiden University Medical Center, Leiden, The Netherlands

<sup>4</sup>Department of Medical Microbiology, University Medical Center Utrecht, Utrecht University, Utrecht, The Netherlands

<sup>5</sup>Department of Biology, Technion Israel Institute of Technology, Haifa, Israel

## Correspondence

Linde Meyaard, Center for Translational Immunology, University Medical Center Utrecht, Utrecht University, Lundlaan 6, 3584 EA Utrecht, The Netherlands.  
Email: l.meygaard@umcutrecht.nl

## Present address

Nina M. van Sorge, Department of Medical Microbiology and Infection Prevention, Netherlands Reference Laboratory for Bacterial Meningitis, Amsterdam Institute for Infection and Immunity, Amsterdam UMC, Location Amsterdam Medical Center, University of Amsterdam, Amsterdam, The Netherlands

## Funding information

Nederlandse Organisatie voor Wetenschappelijk Onderzoek (NWO), Grant/Award Number: 91815608

## Abstract

Signal inhibitory receptor on leukocytes-1 (SIRL-1) is a negative regulator of myeloid cell function and dampens antimicrobial responses. We here show that different species of the genus *Staphylococcus* secrete SIRL-1-engaging factors. By screening a library of single-gene transposon mutants in *Staphylococcus aureus*, we identified these factors as phenol-soluble modulins (PSMs). PSMs are amphipathic  $\alpha$ -helical peptides involved in multiple aspects of staphylococcal virulence and physiology. They are cytotoxic and activate the chemotactic formyl peptide receptor 2 (FPR2) on immune cells. Human cathelicidin LL-37 is also an amphipathic  $\alpha$ -helical peptide with antimicrobial and chemotactic activities, structurally and functionally similar to  $\alpha$ -type PSMs. We demonstrate that  $\alpha$ -type PSMs from multiple staphylococcal species as well as human cathelicidin LL-37 activate SIRL-1, suggesting that SIRL-1 recognizes  $\alpha$ -helical peptides with an amphipathic arrangement of hydrophobicity, although we were not able to show direct binding to SIRL-1. Upon rational peptide design, we identified artificial peptides in which the capacity to ligate SIRL-1 is segregated from cytotoxic and FPR2-activating properties, allowing specific engagement of SIRL-1. In conclusion, we propose staphylococcal PSMs and human LL-37 as a potential new class of natural ligands for SIRL-1.

## KEYWORDS

cathelicidin LL-37, phenol-soluble modulin, SIRL-1, *Staphylococcus*

**Abbreviations:** DAMP, damage-associated molecular pattern; FPR2, formyl peptide receptor 2; LAIR-1, leukocyte-associated immunoglobulin-like receptor 1; LDH, lactate dehydrogenase; NFAT, nuclear factor of activated T cells; NTML, Nebraska transposon mutant library; PAMP, pathogen-associated molecular pattern; PMA, phorbol 12-myristate 13-acetate; PRR, pattern recognition receptor; PSM, phenol-soluble modulin; QS, quorum sensing; SIRL-1, signal inhibitory receptor on leukocytes-1.

<sup>†</sup>Deceased.

This is an open access article under the terms of the Creative Commons Attribution-NonCommercial License, which permits use, distribution and reproduction in any medium, provided the original work is properly cited and is not used for commercial purposes.

© 2021 The Authors. *The FASEB Journal* published by Wiley Periodicals LLC on behalf of Federation of American Societies for Experimental Biology

## 1 | INTRODUCTION

Our defense system typically recognizes microbes through pattern recognition receptors (PRRs), which interact with pathogen-associated molecular patterns (PAMPs).<sup>1</sup> Besides extrinsic stimuli such as bacteria, endogenous damage- or danger-associated molecular patterns (DAMPs) such as defensins, heat shock proteins, cathelicidin LL-37, and some S100 proteins also interact with PRRs and initiate or potentiate immune responses.<sup>2,3</sup> Nevertheless, excessive triggering of PRRs and other activating immune receptors can lead to immune system overactivation, induce immunopathology, and cause tissue damage. To prevent disproportionate activation, inhibitory immune receptors control the activation of immune cells. They dampen and provide context to activation signals that immune cells receive when encountering a microbial or endogenous trigger and raise the activation threshold.<sup>4</sup>

Signal inhibitory receptor on leukocytes-1 (SIRL-1) is an inhibitory immune receptor expressed on granulocytes and monocytes in the blood<sup>5</sup> and monocytes in the lung.<sup>6</sup> A genetic polymorphism regulating SIRL-1 expression levels on monocytes is associated with the inflammatory skin disease atopic dermatitis.<sup>7</sup> Upon SIRL-1 engagement, two immunoreceptor tyrosine-based inhibitory motifs in its cytoplasmic domain become phosphorylated and recruit Src homology 2 domain-containing tyrosine phosphatases 1 and 2 to relay inhibitory signals.<sup>8</sup> Neutrophils possess potent mechanisms for microbe recognition and clearance and are critical immune cells in the defense against bacteria. We have shown that SIRL-1 engagement on neutrophils dampens reactive oxygen species production and neutrophil extracellular trap formation.<sup>8-10</sup> Recently, we have revealed that SIRL-1 is engaged by the endogenous S100 protein family of DAMPs.<sup>11</sup> We have also demonstrated that SIRL-1 is downregulated on in vitro-activated neutrophils<sup>8</sup> and neutrophils present at the site of infection.<sup>12</sup> Therefore, we have proposed that SIRL-1 acts as a disinhibition receptor: once the threshold for activation provided by SIRL-1 is passed, SIRL-1 downregulation allows for the rapid deployment of neutrophil effector mechanisms.<sup>4</sup>

The human skin is covered with a variety of microbes that provide benefit to the host.<sup>13</sup> However, potentially pathogenic microbes are also commonly present among healthy microbiota communities and can, depending on the location or context in which they appear, cause infections.<sup>14</sup> To prevent infections, a robust first line of microbe-controlling mechanisms, such as the skin's acidity, low moisture content, and the production of antimicrobial peptides such as  $\beta$ -defensins, dermcidin, some S100 proteins, and cathelicidin LL-37, is established in the skin.<sup>15-19</sup> The skin-residing Gram-positive bacteria of

the genus *Staphylococcus* are particularly well adapted to life under such conditions.<sup>15,16</sup> *Staphylococcus* comprises bacterial species with vastly different pathogenic potential. The well-characterized *Staphylococcus aureus* can exhibit a commensal-like lifestyle, and commonly colonizes the human nares and skin.<sup>20,21</sup> It is often present on the skin of patients with atopic dermatitis.<sup>22</sup> *S. aureus* is also a well-known pathogen,<sup>20</sup> causing skin and soft tissue infections and even invasive systemic infections.<sup>23,24</sup> *Staphylococcus epidermidis* fulfills a similar dual role in its interaction with the host. It is the most common colonizer of human skin, but can also cause disease, although generally in a hospital setting and not in healthy individuals.<sup>25-27</sup> Many well-characterized virulence factors that increase staphylococcal pathogenicity and promote survival when encountering the host's defense mechanisms have been described, predominantly in *S. aureus*.<sup>28-31</sup> In contrast, features or molecules that promote staphylococcal commensalism are less well understood. Similarly, host factors contributing to the maintenance of tolerance to microbes are mainly unknown. Multiple inhibitory immune receptors interact with microbes.<sup>32</sup> Here, we investigated the SIRL-1 engagement by *Staphylococcus* and identified a new group of staphylococcal and endogenous ligands for SIRL-1.

## 2 | MATERIALS AND METHODS

### 2.1 | Bacterial strains and plasmids

Bacterial strains and plasmids used are described in Tables 1 and 2, respectively. All strains were grown overnight in tryptic soy broth (T8907, Sigma-Aldrich, St. Louis, Missouri, USA) at 37°C with agitation. Plasmid-harboring strains were grown in tryptic soy broth supplemented with 25  $\mu$ g/ml tetracycline (T7660, Sigma-Aldrich, St. Louis, Missouri, USA) overnight at 37°C with agitation. The next day, bacterial cultures were centrifuged for 3 min at 2700 g, and the supernatant was filtered through a 0.2  $\mu$ m filter. Strains of the Nebraska transposon mutant library (NTML) screening array were grown in 900  $\mu$ l tryptic soy broth supplemented with 5  $\mu$ g/ml erythromycin (E5389, Sigma-Aldrich, St. Louis, Missouri, USA) in deep 96-well plates overnight at 37°C without agitation. The next day, bacterial cultures were centrifuged for 3 min at 2700 g, and the supernatant was collected without filtration.

### 2.2 | Peptide design and analysis

We designed twenty-eight 18 AA residue long peptides comprising only amino acids with the highest  $\alpha$ -helical

propensities: lysine as a positively charged, glutamic acid as a negatively charged, glutamine as a polar uncharged, and leucine as a hydrophobic amino acid.<sup>38</sup> Sequence alignment was performed with Clustal Omega,<sup>39</sup> secondary structure prediction was performed with Jpred4,<sup>40</sup> and screening of peptides for specific  $\alpha$ -helical properties was performed with HeliQuest.<sup>41</sup> The 28 designed peptides are shown in Table 3.

**TABLE 1** Bacterial strains used in this study

Bacterial strains	Source
<i>S. aureus</i> LAC wt	[33]
<i>S. aureus</i> LAC $\Delta$ agr	[33]
<i>S. aureus</i> LAC $\Delta$ PSM	[34]
<i>S. aureus</i> LAC $\Delta$ PSM $\alpha$ 1-4	[33]
<i>S. aureus</i> LAC $\Delta$ PSM $\beta$ 1-2	[33]
<i>S. aureus</i> LAC $\Delta$ hld	[33]
<i>S. aureus</i> MW2 wt	[33]
<i>S. aureus</i> MW2 $\Delta$ agr	[33]
<i>S. aureus</i> MW2 $\Delta$ PSM	[35]
<i>S. aureus</i> MW2 $\Delta$ PSM $\alpha$ 1-4	[33]
<i>S. aureus</i> MW2 $\Delta$ PSM $\beta$ 1-2	[33]
<i>S. aureus</i> MW2 $\Delta$ hld	[33]
<i>S. epidermidis</i> ATCC 49134	Own
<i>S. capitis</i> ATCC 35661	Own
<i>S. carnosus</i> TM-300	Own
<i>S. haemolyticus</i> KV-116	Own
<i>S. hominis</i> KV-111	Own
<i>S. warneri</i> KV-112	Own
<i>S. saprophyticus</i> ATCC 35552	Own
<i>S. lugdunensis</i> M23590, HM-141 <sup>a</sup>	NIAID, NIH
<i>S. caprae</i> C87, HM-246 <sup>b</sup>	NIAID, NIH
Nebraska transposon mutant library (NTML), NR-48501 <sup>c</sup>	NIAID, NIH

<sup>a</sup>Provided by BEI Resources, NIAID, NIH, as part of the Human Microbiome Project.

<sup>b</sup>Provided by NIH Biodefense and Emerging Infections Research Resources Repository, NIAID, NIH, as part of the Human Microbiome Project.

<sup>c</sup>Provided by the Network on Antimicrobial Resistance in *Staphylococcus aureus* (NARSA) for distribution by BEI Resources, NIAID, NIH.

**TABLE 2** Plasmids used in this study

Plasmids	Description	Source
pTX $\Delta$ 16	Tetracycline (Tet) resistance, control plasmid	[33]
pTX $\Delta$ 16-PSM $\alpha$	Tet resistance, <i>psma</i> 1-4 genes constitutively expressed through xylose promoter	[33]
pTX $\Delta$ 16-PSM $\beta$	Tet resistance, <i>psm</i> $\beta$ 1-2 genes constitutively expressed through xylose promoter	[36]
pTX $\Delta$ 16-hld	Tet resistance, <i>hld</i> gene constitutively expressed through xylose promoter	[37]

## 2.3 | Peptide synthesis

*S. aureus* PSM $\alpha$ 3, N'-formyl-PSM $\alpha$ 3, C'-N' reversed sequence PSM $\alpha$ 3, all-D-PSM $\alpha$ 3, N'-formyl- $\delta$ -toxin, and N'-formyl-PSM $\beta$ 1<sup>33</sup> were custom synthesized by GenScript (Piscataway, New Jersey, USA) at 95% purity. Human cathelicidin LL-37<sup>42</sup> was custom synthesized by GenScript (Piscataway, New Jersey, USA) at 95% purity or purchased from AnaSpec (AS-61302, AnaSpec, Fremont, California, USA). *S. aureus* PSM $\alpha$ 1, PSM $\alpha$ 2, PSM $\alpha$ 4, PSM $\beta$ 1-2,  $\delta$ -toxin,<sup>33</sup>  $\delta$ -toxin allelic variant G10S,<sup>43</sup> PSM-Mec,<sup>44</sup> N-AgrD F20, N-AgrD F24 and N-AgrD D20,<sup>45</sup> *S. epidermidis* PSM $\alpha$ , PSM $\beta$ 1-3, PSM $\gamma$ / $\delta$ -toxin, PSM $\delta$  and PSM $\epsilon$ ,<sup>46,47</sup> *Staphylococcus haemolyticus* PSM $\alpha$  and PSM $\beta$ 1-3,<sup>48</sup> *Staphylococcus lugdunensis* PSM $\epsilon$ <sup>49</sup> and OrFX,<sup>50</sup> *Staphylococcus pseudintermedius* PSM $\epsilon$ , *Staphylococcus warneri* PSM $\epsilon$ ,<sup>45</sup> and all 28 designed peptides were synthesized in-house precisely as described before.<sup>11</sup> Peptide sequences are available in the listed references and Table 3.

## 2.4 | Antibody generation

Mouse anti-human-SIRL-1 antibody clone 3D3 was generated as described previously.<sup>5</sup> BALB/c mice were subcutaneously injected with 50  $\mu$ g SIRL-1 ectodomain (in-house production, as described in Ref. [5]), and injections were repeated 2 and 3 weeks after the first injection. Mice were sacrificed 3 days after the final injection, and we fused splenic PBMCs with SP2/0 cells using standard hybridoma technology. We screened the resulting hybridoma clones for specific binding to SIRL-1-transfected RBL-2H3 cells. We obtained monoclonal hybridoma cells by performing limiting dilution, screened them again for SIRL-1 binding, and selected clone 3D3 as a prominent SIRL-1 binder. We purified the mAb clone 3D3 from the monoclonal hybridoma cell supernatant using a HiTrap Protein G HP column (17-0405-01, GE Life sciences, Fairfield, Connecticut, USA).

TABLE 3 Sequences of the 28 designed peptides

No. peptide	Sequence	No. peptide	Sequence
1	LQLLQQLLQQLQQLLQQL	15	LQLLKQLLKKLKKLLQKL
2	LQLQLQLQLQLQLQLQLQ	16	LQLLKQLLKKLQKLLQKL
3	LQLEKLLLEKLEKELLKEL	17	LQLLKQLLQKQLKLLQKL
4	LQLELELEKLELELEKLEK	18	LQLLKQLLQKQLLQQLQKL
5	LKLLKLLKLLKLLKLLKLL	19	LQLLKQLLQQLQQLLQKL
6	LKLLKLLKLLKLLKLLKLL	20	LQLLKQLLQQLQQLLQQL
7	LELELELELELELELELE	21	LQLEQLLQQLQQLLQQL
8	ELELELELELELELELELE	22	LQLEQLLQQLQQLLQEL
9	QKQKQKQKQKQKQKQKQ	23	LQLEQLLEQLQQLLQEL
10	QKQKQKQKQKQKQKQKQ	24	LQLEQLLEQLQELLQEL
11	QEQEEQEEQEEQEEQEEQ	25	LQLEQLLEELQELLQEL
12	EQEQEQEQEQEQEQEQEQ	26	LQLEQLLEELEELLQEL
13	LQLLKKLLKLLKLLKLLKLL	27	LQLEELLELELEELLQEL
14	LQLLKKLLKLLKLLKLLQKL	28	LQLEELLELELELELEEL

## 2.5 | 2B4 NFAT-GFP reporter cell assay

The 2B4 cell line is a T-cell hybridoma cell line. In the 2B4 NFAT-GFP reporter cell lines, extracellular domains of human leukocyte-associated immunoglobulin-like receptor 1 (LAIR-1) and SIRT-1 are fused to the transmembrane and intracellular domains of human CD3 $\zeta$ .<sup>11,51</sup> Ligation of either the cells' endogenous CD3 $\zeta$  or a hLAIR-1-CD3 $\zeta$  or hSIRT-1-CD3 $\zeta$  chimera by an antibody or a ligand results in nuclear factor of activated T-cells (NFAT) promoter-driven GFP expression. Reporter cells were maintained in RPMI 1640 (52400-041, Life Technologies, Carlsbad, California, USA) supplemented with 10% heat-inactivated fetal bovine serum (Biowest, Nuaille, France) and 50 U/ml penicillin-streptomycin (11528876, Life Technologies, Carlsbad, California, USA) (referred to as culture medium hereafter). The NFAT-GFP reporter cell assay was performed with wt-CD3 $\zeta$ , hSIRT-1-CD3 $\zeta$ , or hLAIR-1-CD3 $\zeta$  NFAT-GFP reporter cells. Nunc MaxiSorp (442404, ThermoFisher Scientific, Waltham, Massachusetts, USA) (Figures 1-4, 5A,B) or Greiner Bio-One (655101, Kremsmünster, Austria) (Figure 5C) 96-well flat-bottom plates were coated overnight at 4°C with overnight bacterial supernatants, synthetic peptides, and controls (50  $\mu$ l per well). Mouse anti-human-SIRT-1 mAb (clone 1A5, in-house; 10  $\mu$ g/ml), mouse anti-human-LAIR-1 mAb (clone 8A8, in-house; 10  $\mu$ g/ml), Armenian hamster anti-mouse-CD3 (clone 145-2C11; 10  $\mu$ g/ml; BD, Franklin Lakes, New Jersey, USA) in PBS (D8537, Sigma-Aldrich, St. Louis, Missouri, USA), and human collagen I (CC050, Sigma-Aldrich, St. Louis, Missouri, USA) 2 mM acetic acid (A6283, Merck, Darmstadt, Germany; 5  $\mu$ g/ml) were used as controls. The next day, wells were washed three

times with PBS, and  $0.5 \times 10^4$  reporter cells in 200  $\mu$ l culture medium were seeded to each well. Plates were incubated overnight in a cell culture incubator at 37°C and 5% CO<sub>2</sub>. Where indicated, reporter cells were pre-incubated with mouse-anti-SIRT-1 clones 1A5 or 3D3 or mouse-anti-LAIR-1 clone 8A8 for 30 min before seeding to the plate without washing. For the anti-CD3 mAb control in reporter assays with pre-incubation with antibodies, 1  $\mu$ g/ml anti-mouse-CD3 was coated to the plate. The next day, GFP expression was measured by flow cytometry (LSR Fortessa; BD Bioscience, Franklin Lakes, New Jersey, USA) and analyzed with FlowJo software (version 10.0.7r2).

## 2.6 | 2B4 NFAT translocation assay

hSIRT-1-CD3 $\zeta$  reporter cells were stimulated for 30 min on 96-well MaxiSorp flat-bottom plates coated overnight at 4°C with PSM $\alpha$ 3, LL-37, or the same control antibodies as were used in the 2B4 NFAT-GFP reporter assay. In addition, cells were stimulated with 50 ng/ml phorbol 12-myristate 13-acetate (PMA; P8139, Sigma-Aldrich, St. Louis, Missouri, USA) and 3.75  $\mu$ M ionomycin (I0634, Sigma-Aldrich, St. Louis, Missouri, USA). After 30 min, cells were fixed by a 15-minute incubation in 3.7% paraformaldehyde (F8773, Sigma-Aldrich, St. Louis, Missouri, USA). Cells were then washed three times with PBS with 1% bovine serum albumin (BSA; BSAV-RO, Roche, Basel, Switzerland) and stained with DRAQ5 (424101, BioLegend, San Diego, California, USA) and an anti-NFAT mAb (conjugated to Alexa Fluor488, clone D43B1; 14324S, Cell Signaling, Danvers, Massachusetts, USA), diluted in



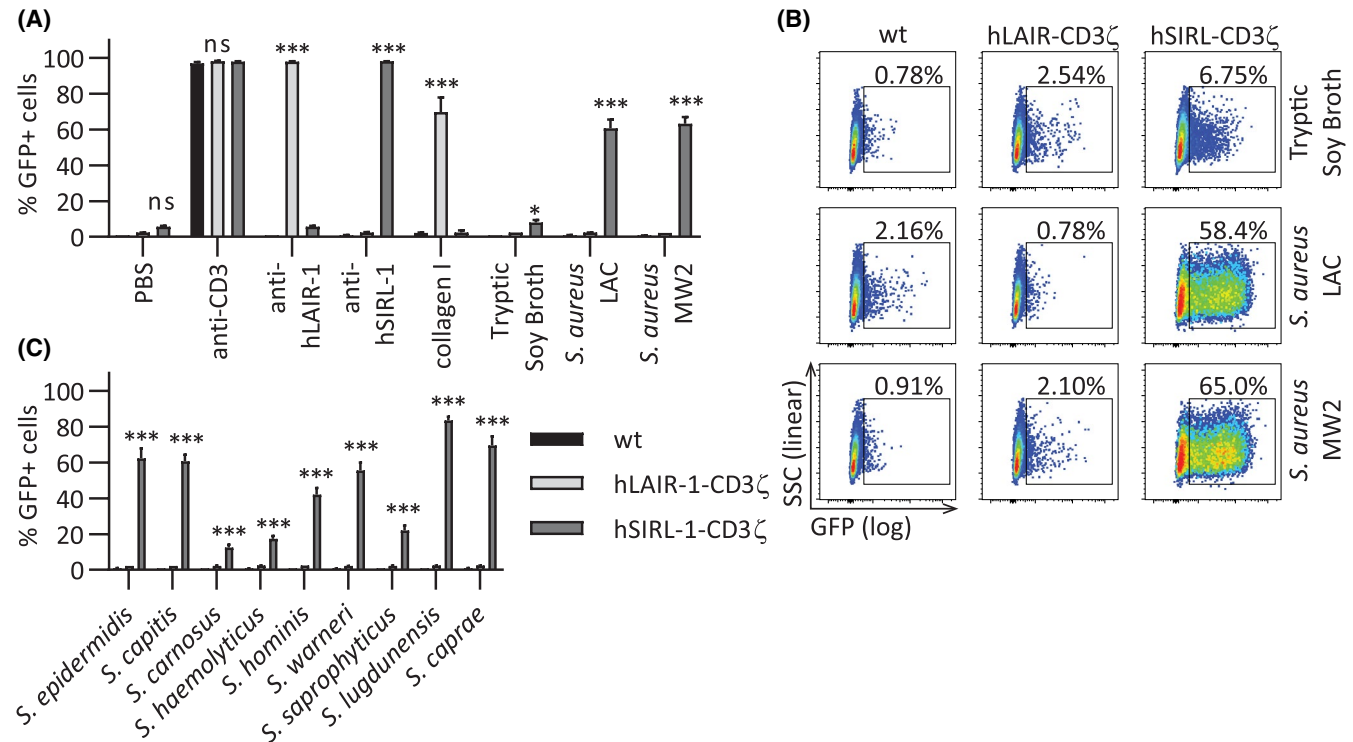


**FIGURE 1** Supernatants of different staphylococcal species activate SIRT-1. Wild-type, hLAIR-1-CD3 $\zeta$ -, or hSIRT-1-CD3 $\zeta$ -expressing NFAT-GFP reporter cells were stimulated overnight with plate-coated control antibodies, collagen, tryptic soy broth, or supernatants of overnight cultures of different *Staphylococcus sp.* grown in tryptic soy broth. GFP expression upon overnight stimulation was measured by flow cytometry. (A) The percentage of GFP-positive reporter cells in response to stimulation with plate-coated PBS (negative control), anti-mouse CD3-, anti-LAIR-1-, and anti-SIRT-1-specific antibodies, the LAIR-1 ligand collagen (positive controls), and overnight culture supernatants of the *Staphylococcus aureus* strains LAC and MW2 and tryptic soy broth as control. (B) Representative dot plots showing the percentage of GFP-positive reporter cells after stimulation with *S. aureus* strains LAC and MW2, with tryptic soy broth as control. (C) The percentage of GFP-positive reporter cells in response to stimulation with plate-coated supernatants of nine other staphylococcal species. Mean and SD of three independent experiments are displayed. Student's *t*-test with the Holm-Šidák multiple-comparison correction. Significance is indicated for the comparison of hLAIR-1-CD3 $\zeta$  to hSIRT-1-CD3 $\zeta$ . \**p* < .05; \*\**p* < .01; \*\*\**p* < .001; ns = not significant

PBS with 1% BSA and 0.1% Triton X-100 (X100, Sigma-Aldrich, St. Louis, Missouri, USA). After three washes with PBS with 1% BSA, NFAT translocation was measured by imaging flow cytometry (ImageStream; Amnis, Austin, Texas, USA). Data were analyzed using the IDEAS software (Amnis, Austin, Texas, USA). Nuclear translocation of NFAT was assessed by analyzing the overlay between the nuclear signal (DRAQ5) and NFAT (Alexa Fluor488). We reported the percentage of the cells with a DRAQ5-Alexa Fluor488 similarity score above 2.5 (as assessed by the Similarity Feature in IDEAS software) as the percentage of cells with nuclear NFAT.

## 2.7 | Lactate dehydrogenase (LDH) release cytotoxicity assay

LDH release cytotoxicity assay was performed using the Pierce LDH Cytotoxicity Assay Kit (88953, ThermoFisher

Scientific, Waltham, Massachusetts, USA). hSIRT-1-CD3 $\zeta$  GFP reporter cells were routinely cultured as described above. For the LDH assay, cells were transferred to RPMI 1640 without phenol red (11835063, ThermoFisher Scientific, Waltham, Massachusetts, USA) supplemented with 5% heat-inactivated fetal bovine serum and seeded to a flat-bottom 96-well plate at 20 000 cells per well in 100  $\mu$ l medium. Cells were incubated overnight in a cell culture incubator at 37°C and 5% CO<sub>2</sub>. The next day, 10  $\mu$ l of peptides dissolved in water was added to the cells to a final concentration of 10  $\mu$ M. Water and manufacturer-provided lysis buffer were used as controls. Cells were incubated in a cell culture incubator at 37°C and 5% CO<sub>2</sub> for 45 min. After incubation, supernatants were collected, and the detection of LDH was performed following the manufacturer's instructions. Absorbance at 490 and 680 nm was measured. The 680 nm absorbance values were subtracted from the 490 nm absorbance values. Values were normalized to

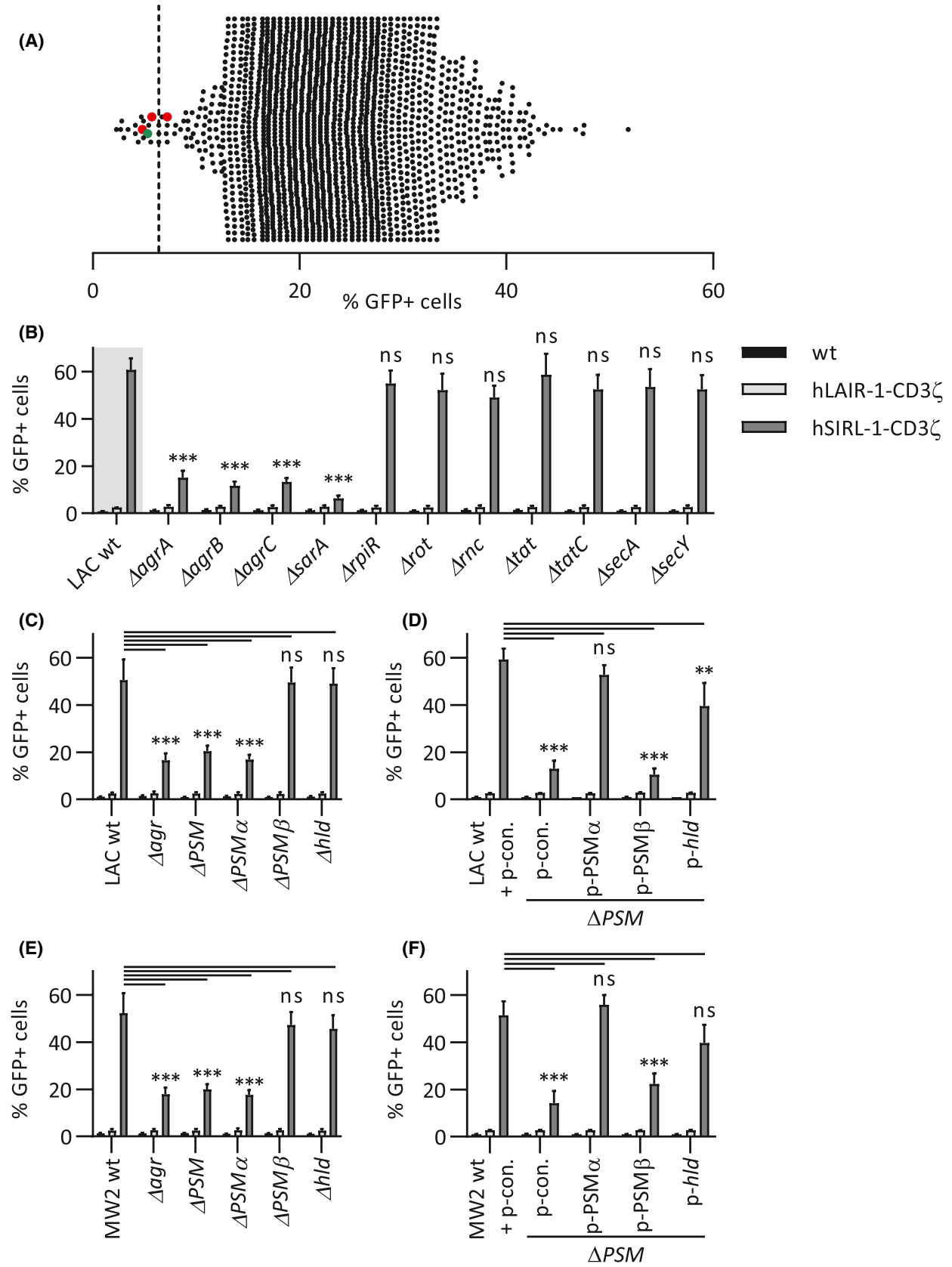


**FIGURE 2** Inactivation of genes encoding phenol-soluble modulins  $\alpha$ 1-4 and  $\delta$ -toxin (*hld*) in *Staphylococcus aureus* abrogates its ability to activate SIRL-1. Wild-type, hLAIR-1-CD3 $\zeta$ , or hSIRL-1-CD3 $\zeta$ -expressing NFAT-GFP reporter cells were stimulated overnight with plate-coated overnight supernatants of *S. aureus* strains. GFP expression upon overnight stimulation was measured by flow cytometry. (A) Supernatants of all *S. aureus* single-gene transposon (Tn) insertion mutants in the Nebraska transposon mutant library (NTML) were screened for activation of the hSIRL-1-CD3 $\zeta$  reporter cell line. Each dot represents the GFP expression induced by the supernatant of an individual mutant in the library. Inactivation of *S. aureus* genes *agrABC* (red dots) and *sarA* (green dot) and tryptic soy broth-induced background (dashed line) are highlighted. (B) NTML Tn-insertion mutants of *sarA* and *agrABC*, along with mutants of two major protein secretion systems: *tat/tatC* and *secA/secY*, and mutants of regulators of *S. aureus* gene expression *rpiR*, *rot*, and *rnc* were retested in the GFP reporter cell assay. Significance is indicated for the comparison of hSIRL-1-CD3 $\zeta$  stimulated with supernatant of mutant bacteria to hSIRL-1-CD3 $\zeta$  stimulated with supernatant of *S. aureus* LAC wt (result from Figure 1, here plotted for comparison and shaded grey). (C, E) Supernatants of isogenic deletion mutants in all four *agrABCD* quorum sensing system-encoding genes ( $\Delta$ *agr*), the triple deletion mutant ( $\Delta$ PSM) in all PSM-encoding genes (PSM $\alpha$ 1-4, PSM $\beta$ 1-2, and  $\delta$ -toxin *hld*), and mutants in genes encoding  $\alpha$ -type PSMs ( $\Delta$ PSM $\alpha$ ),  $\beta$ -type PSMs ( $\Delta$ PSM $\beta$ ), and  $\delta$ -toxin ( $\Delta$ *hld*) were tested in the GFP reporter cell assay. Deletion mutants in *S. aureus* LAC (C) and *S. aureus* MW2 (E) genetic backgrounds were used. (D, F) Supernatants of the triple PSM deletion strain ( $\Delta$ PSM) with re-introduced plasmid-encoded PSM $\alpha$ 1-4 (p-PSM $\alpha$ ) or PSM $\beta$ 1-2 (p-PSM $\beta$ ) or  $\delta$ -toxin (p-*hld*) genes were tested in the GFP reporter cell assay. Plasmid complementation was done in  $\Delta$ PSM mutants of *S. aureus* LAC (D) and MW2 (F). Significance is indicated for the comparison of hSIRL-1-CD3 $\zeta$  stimulated with knockouts (C, E) or plasmid-complemented strains (D, F) to hSIRL-1-CD3 $\zeta$  stimulated with wt strains (C, E) or strains complemented with control plasmid (D, F). Mean and SD of three independent experiments are displayed in panels B-F. One-way ANOVA followed by Dunnett's multiple-comparisons test. \* $p < .05$ ; \*\* $p < .01$ ; \*\*\* $p < .001$ ; ns = not significant

water-treated cells as 0% cytotoxicity and lysis-buffer-treated cells as 100% cytotoxicity. The experiment was performed in duplicates.

## 2.8 | Formyl peptide receptor 2 (FPR2)-mediated Ca<sup>2+</sup> mobilization assay

HL-60 FPR2 cells<sup>52</sup> were routinely cultured in culture medium (described above). Prior to the assay, cells were transferred to RPMI 1640 without phenol red supplemented with 1% BSA and 50 U/ml penicillin-streptomycin (assay medium). To assess FPR2 activation, we measured FPR2-specific Ca<sup>2+</sup> fluxes. HL-60 FPR2 cells were washed twice with assay medium.  $1.5 \times 10^6$  cells in 1.5 ml medium were mixed with 5  $\mu$ M Fluo-3-AM (F14218, Invitrogen, Waltham, Massachusetts, USA) dissolved in DMSO (472301, Sigma-Aldrich, St. Louis, Missouri, USA) and incubated in a cell culture incubator at 37°C and 5% CO<sub>2</sub> for 30 min. After incubation, cells were washed with assay medium and resuspended to a final concentration of  $2 \times 10^6$  cells per ml. To block FPR2, we added 15  $\mu$ M WRW4 peptide (2262/1, Tocris Bio-Techne, Minneapolis, Minnesota, USA) dissolved in H<sub>2</sub>O to the cells. Five hundred  $\mu$ l of cell suspension was pipetted into FACS tubes. Ca<sup>2+</sup> fluxes were recorded by FACS (FACSCanto II, BD Bioscience, Franklin Lakes, New Jersey, USA) using a 488 nm excitation laser and 530/30 nm filter. The baseline signal was measured for 30 s. Next, peptides were added to the cells to a 1.5  $\mu$ M final concentration, cells were very briefly vortexed, and Ca<sup>2+</sup> fluxes were immediately recorded for up to 4 min. FlowJo (version 10.0.7r2) kinetics platform was used for initial data analysis. A time series of median fluorescence values were exported for every sample. Baseline ( $I_0$ ) was established as the average signal

of the first 25 s of measurement, and data were normalized using the formula  $(I - I_0)/I_0$ . Unless stated otherwise, maximum signals after stimulation are reported.

## 2.9 | Statistical analysis

Student's *t*-test with the Holm-Šidák multiple-comparison correction or one-way ANOVA followed by Dunnett's or Tukey's multiple-comparisons test were performed as indicated. *p*-values lower than .05 were considered statistically significant (\* $p < .05$ ; \*\* $p < .01$ ; \*\*\* $p < .001$ ). Statistical analysis was performed with GraphPad Prism 8.

## 3 | RESULTS

### 3.1 | SIRL-1 is engaged by a factor secreted by staphylococci

We used 2B4 NFAT-GFP reporter cells, additionally expressing a chimeric protein consisting of the extracellular domain of human SIRL-1 and the transmembrane region and intracellular domain of CD3 $\zeta$  (hSIRL-1-CD3 $\zeta$ ) to screen for potential bacterial ligands for SIRL-1. As controls, we used non-transduced and hLAIR-1-CD3 $\zeta$ -transduced 2B4 NFAT-GFP reporter cells. We stimulated all three NFAT-GFP reporter cell lines with plate-coated specific monoclonal antibodies against mouse CD3, hLAIR-1 (clone 8A8) or hSIRL-1 (clone 1A5), or collagen I. All three cell lines highly expressed GFP upon stimulation with anti-mouse CD3, which ligates the endogenous mouse CD3 protein expressed by the 2B4 NFAT-GFP cell line (Figure 1A). Stimulation with anti-LAIR-1 and anti-SIRL-1 antibodies induced

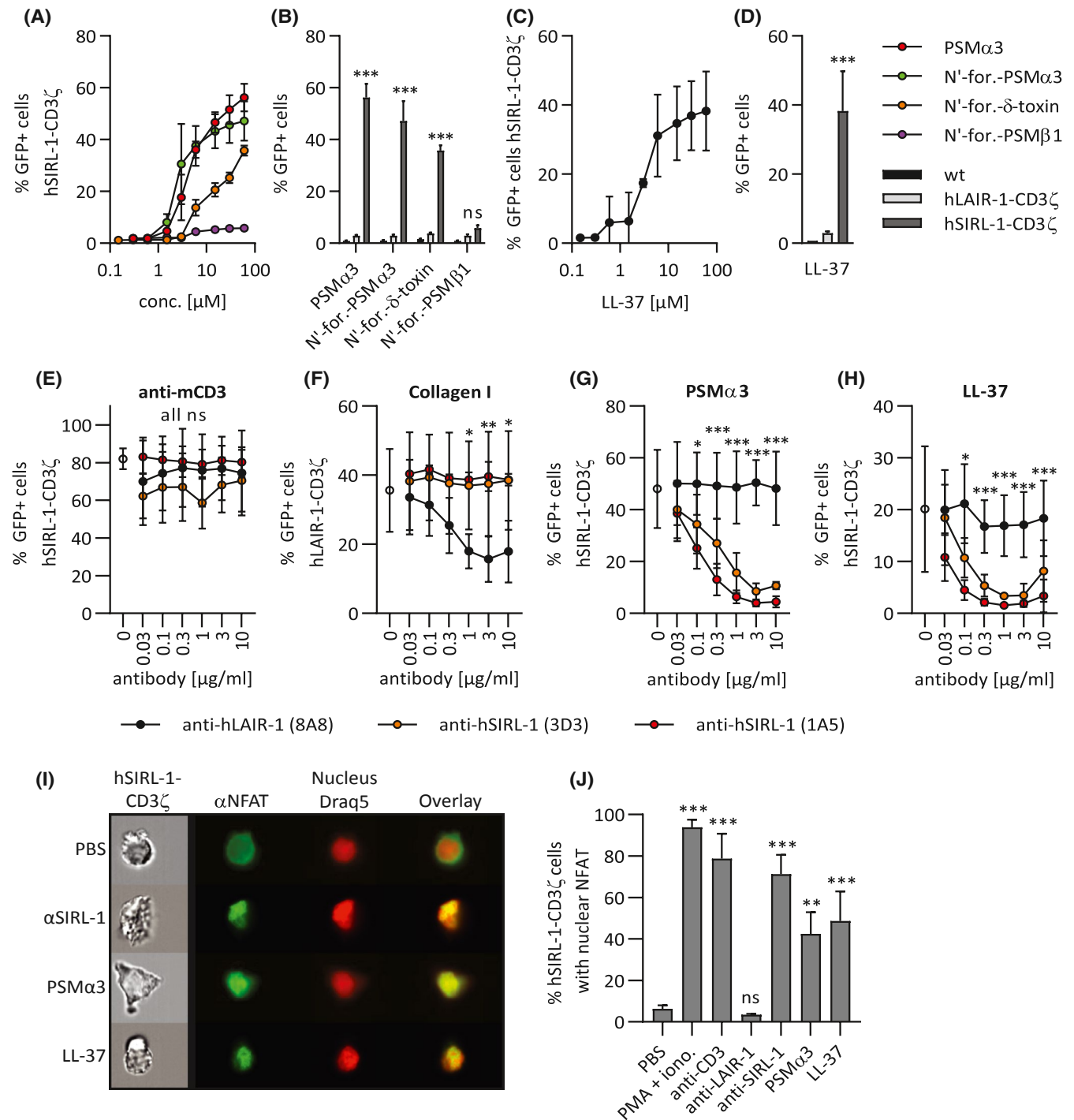


**FIGURE 3** Synthetic *Staphylococcus aureus* PSM $\alpha$ 3 and  $\delta$ -toxin and human cathelicidin LL-37 selectively activate SIRL-1. (A–D) Wild-type, hLAIR-1-CD3 $\zeta$ , or hSIRL-1-CD3 $\zeta$ -expressing NFAT–GFP reporter cells were stimulated overnight with a concentration range of up to 60  $\mu$ M of plate-coated PSM $\alpha$ 3, N'-formylated PSM $\alpha$ 3, N'-formylated PSM $\beta$ 1, and N'-formylated  $\delta$ -toxin of *S. aureus* (A) and human cathelicidin LL-37 (C), as indicated. In B and D, only stimulations with 60  $\mu$ M plate-coated peptides are shown for all three reporter cell lines. (E–H) hLAIR-1-CD3 $\zeta$ - or hSIRL-1-CD3 $\zeta$ -expressing NFAT–GFP reporter cells were pre-incubated with anti-hLAIR-1 and two different anti-hSIRL-1 antibodies, and then stimulated overnight with plate-coated anti-mCD3 (E), collagen I (F), PSM $\alpha$ 3 (G), or LL-37 (H) as indicated. GFP expression upon stimulation was measured by flow cytometry (A–H). (I, J) Visualization (I) and quantification (J) of NFAT translocation into the nucleus 30 min after stimulation of the hSIRL-1-CD3 $\zeta$  GFP reporter cell line with PBS, phorbol 12-myristate 13-acetate and ionomycin (PMA + iono.), and plate-coated anti-CD3, anti-LAIR-1, anti-SIRL-1, PSM $\alpha$ 3, and cathelicidin LL-37 were assessed by ImageStream. Mean and SD of three independent experiments are displayed. (B, D–H) Student's *t*-test with the Holm–Šidák multiple-comparison correction (no correction in D). (B, D) Significance is indicated for the comparison of hLAIR-1-CD3 $\zeta$  to hSIRL-1-CD3 $\zeta$ . (E–H) Significance is indicated for the comparison of anti-hLAIR-1 (8A8) to anti-hSIRL-1 (1A5) pre-incubation of reporter cells. (J) One-way ANOVA followed by Dunnett's multiple-comparisons test. Significance is indicated for the comparison of PBS to all other conditions. \**p* < .05; \*\**p* < .01; \*\*\**p* < .001; ns = not significant



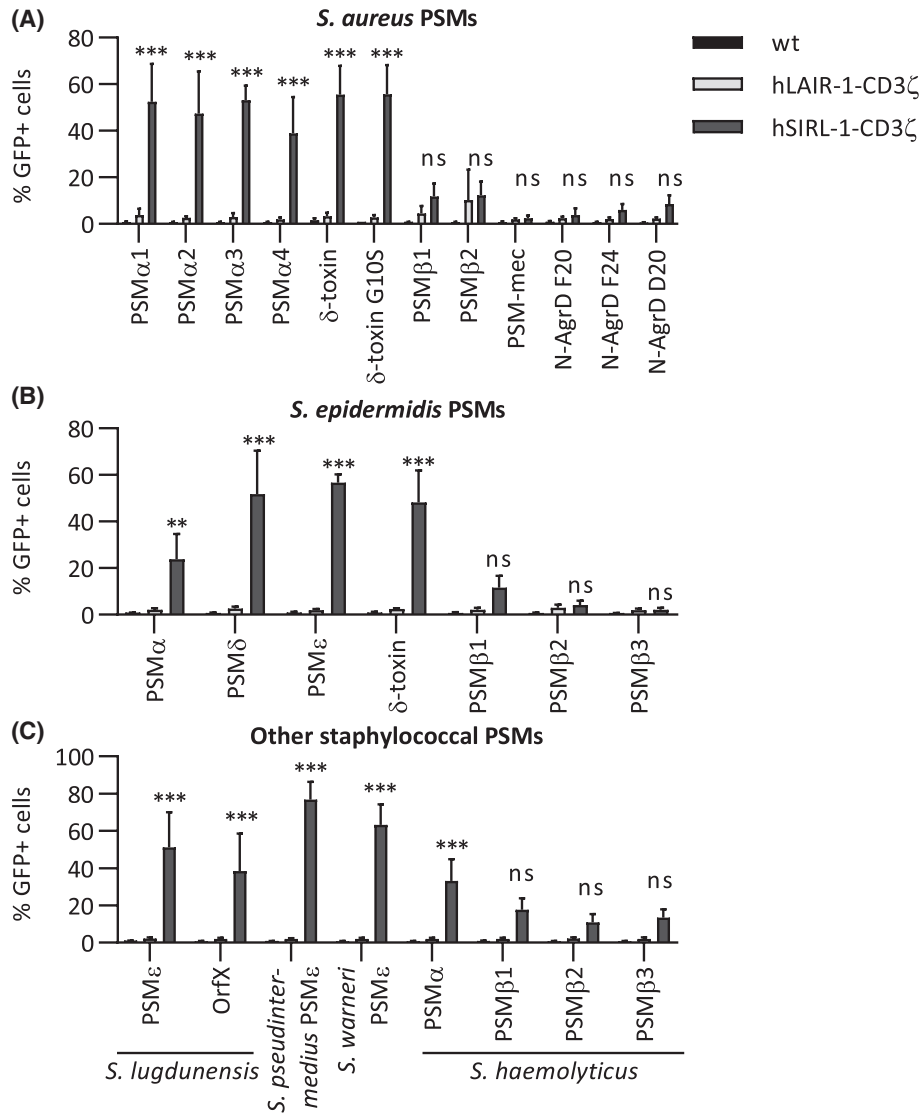


**FIGURE 4** SIRT-1 is activated by  $\alpha$ -type phenol-soluble modulins of multiple staphylococcal species. Wild-type, hLAIR-1-CD3 $\zeta$ - or hSIRT-1-CD3 $\zeta$ -expressing NFAT-GFP reporter cells were stimulated overnight with 10  $\mu$ M plate-coated peptides as indicated. After overnight incubation, GFP expression was measured by flow cytometry. PSMs from (A) *S. aureus*, (B) *S. epidermidis*, and (C) other staphylococci were used, as indicated. Mean and SD of three independent experiments are displayed. Student's *t*-test with the Holm-Šidák multiple-comparison correction. Significance is indicated for the comparison of hLAIR-1-CD3 $\zeta$  to hSIRT-1-CD3 $\zeta$ . \**p* < .05; \*\**p* < .01; \*\*\**p* < .001; ns = not significant

high GFP expression only in the respective cell lines, demonstrating specificity (Figure 1A). Additionally, the hLAIR-1-CD3 $\zeta$  reporter cell line was stimulated with plate-coated collagen I, one of many types of collagens that are natural ligands of LAIR-1,<sup>51</sup> resulting in up to 70% GFP-positive cells (Figure 1A). Next, we stimulated the reporter cell lines with plate-coated overnight supernatants of *S. aureus* strains LAC and MW2. Supernatants from both strains induced GFP expression in hSIRT-1-CD3 $\zeta$  reporter cells, resulting in around 60% GFP-positive cells (Figure 1A,B). We observed no response in hLAIR-1-CD3 $\zeta$  reporter cells, indicating

specificity for SIRT-1 (Figure 1A,B). The bacterial culture broth, tryptic soy broth, induced only minimal GFP expression in the hSIRT-1-CD3 $\zeta$  line (Figure 1A,B). To determine whether the potential SIRT-1 ligand was conserved among other staphylococcal species, we stimulated the reporter cell lines with overnight supernatants of nine additional staphylococcal species (Figure 1C). All supernatants induced GFP expression in hSIRT-1-CD3 $\zeta$  reporter cells, whereas none induced GFP expression in hLAIR-1-CD3 $\zeta$  or wt reporter cells. This shows that a potential bacterial SIRT-1 ligand is conserved among staphylococci.

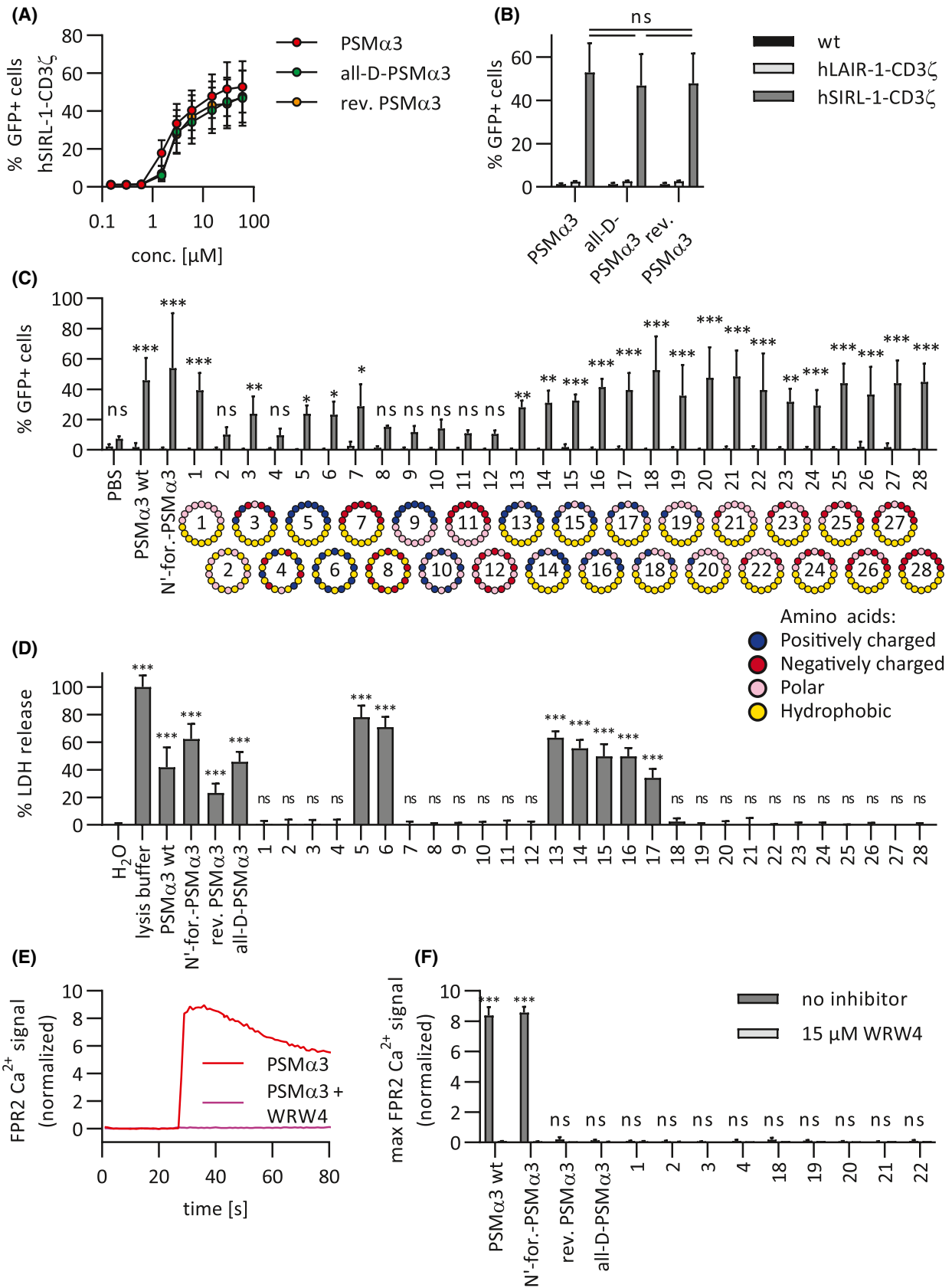


**FIGURE 5** Artificial non-toxic amphipathic peptides specifically activate SIRL-1 and not FPR2. Wild-type, hLAIR-1-CD3 $\zeta$ - or hSIRL-1-CD3 $\zeta$ -expressing NFAT-GFP reporter cells were stimulated overnight with plate-coated peptides. After overnight incubation, GFP expression was measured by flow cytometry. (A, B) Reporter cells were stimulated with a concentration range of up to 60  $\mu$ M of plate-coated PSM $\alpha$ 3, all-D-PSM $\alpha$ 3 composed of D-isomers of amino acids in the same sequence as in the wt PSM $\alpha$ 3, and reverse PSM $\alpha$ 3 in which the amino acid sequence was reversed C'-N'. (A) concentration-dependent activation of hSIRL1-CD3 $\zeta$  cell line. (B) Reporter cells stimulated with 60  $\mu$ M plate-coated peptides from (A). One-way ANOVA followed by Tukey's multiple-comparisons test. Significance is indicated for all comparisons between hSIRL-1-CD3 $\zeta$  conditions. (C) Reporter cell lines were stimulated with a series of 28 artificially designed peptides with varying content and distribution of AA residues with different properties. Their helical wheel representations are shown. Amphipathic peptides contain hydrophobic residues (marked yellow) that partition to one side of the helix. Peptides were plate coated from a 10  $\mu$ M solution. Student's *t*-test with the Holm-Šidák multiple-comparison correction. Significance is indicated for the comparison of hLAIR-1-CD3 $\zeta$  to hSIRL-1-CD3 $\zeta$ . (D) Cytotoxicity of 10  $\mu$ M wt PSM $\alpha$ 3, N'-formylated PSM $\alpha$ 3, C'-N' reverse sequence PSM $\alpha$ 3, all-D-amino acid PSM $\alpha$ 3, and all 28 artificial peptides against the hSIRL-1-CD3 $\zeta$  reporter cells was assessed by measuring LDH release after a 45-minute incubation. One-way ANOVA followed by Dunnett's multiple-comparisons test. Significance is indicated for the comparison of hSIRL-1-CD3 $\zeta$  reporter cells treated with 10  $\mu$ M peptides to hSIRL-1-CD3 $\zeta$  reporter cells treated with H<sub>2</sub>O. (E, F) HL-60 FPR2 cells were stimulated with PSM $\alpha$ 3 and its derivatives, and with a selection of artificial SIRL-1-activating peptides that showed to be non-toxic (C, D). FPR2-mediated Ca<sup>2+</sup> mobilization was monitored by flow cytometry. We stimulated the cells in presence or absence of a specific FPR2 inhibitor WRW4. (E) A representative Ca<sup>2+</sup> signal induced by PSM $\alpha$ 3 wt is shown. (F) Maximum Ca<sup>2+</sup> signals with or without the FPR2 inhibitor are shown for all tested peptides. Student's *t*-test with the Holm-Šidák multiple-comparison correction. Significance is indicated for the comparison of HL-60 FPR2 stimulated with the peptides in presence or absence of WRW4. (A–D, F) Mean and SD of three independent experiments are shown. \**p* < .05; \*\**p* < .01; \*\*\**p* < .001; ns = not significant

### 3.2 | Staphylococcal *agr* operon controls expression of the SIRL-1-activating factor

*S. aureus* is the most intensely studied member of the genus *Staphylococcus*, with a wealth of research tools available to study its biology. To identify the staphylococcal SIRL-1 ligand, we screened the supernatants of all 1920 arrayed *S. aureus* mutants from the NTML for their ability to activate SIRL-1 as measured by induction of GFP expression in the hSIRL-1-CD3 $\zeta$  reporter cells (Figure 2A). Nineteen mutants induced percentages of GFP-positive hSIRL-1-CD3 $\zeta$  reporter cells equal to or lower than the background levels (6.4% GFP-positive reporter cells) induced by tryptic soy broth used to cultivate bacteria (Figure 2A, dashed line). Fifteen of these mutants are mutated in proteins normally not secreted from *S. aureus*, and one is a mutant of a putative membrane protein. These sixteen mutants are listed in the Appendix Table A1, and we excluded them from further analysis. We next focused on the remaining three Tn-insertion mutants that induced percentages of GFP-positive cells lower than the background. Two of these Tn-insertion mutants were mutated in genes *agrB* and *agrC* (4.8% and 5.7% GFP-positive reporter cells, respectively; Figure 2A, red dots below background dashed line), which are part of the *agr* operon. The *agr* operon comprises four genes *agrA*–*agrD*.<sup>53</sup> Additionally, a Tn-insertion mutant in the third gene of the *agr* operon, *agrA*, induced 7.2% GFP-positive reporter cells, which is slightly above background (Figure 2A, red dot above background dashed line), whereas the fourth gene *agrD* is not present in the NTML. The third Tn-insertion mutant of interest was mutated in *sarA* (5.3% GFP-positive reporter cells; Figure 2A, green dot).

The *agr* operon encodes the *S. aureus* quorum sensing (QS) system, which consists of four cooperatively acting proteins AgrA–AgrD and controls the expression of accessory genes such as toxins, adhesins, and other proteins essential for biology and virulence of staphylococci.<sup>53</sup> The gene *sarA* encodes the staphylococcal accessory regulator A (SarA), which controls the transcription of the *agr* operon.<sup>53</sup> AgrD is a small peptide secreted through the cell wall-residing AgrB into the extracellular space, where it accumulates with the increasing density of bacterial population. High concentrations of AgrD activate the cell wall-residing receptor histidine kinase AgrC.<sup>54</sup> Activated AgrC, in turn, phosphorylates the cytoplasmic response regulator AgrA, which in conjunction with SarA initiates transcription from *agr* promoters.<sup>55</sup> Our data show that the *agr* system either regulates the secretion of a potential SIRL-1 ligand in *S. aureus* or that its components themselves induce GFP expression in the SIRL-1 reporter cell line. AgrD is the only one of the four Agr proteins that is not inactivated in the NTML but also the only secreted Agr protein, making it a likely candidate for SIRL-1 activation. In line with this, inactivation of AgrB, which is required for AgrD secretion, results in significant decrease in SIRL-1 activation. Nevertheless, inactivation of AgrA/C also results in abrogation of SIRL-1 activation, and secretion of AgrD is not dependent on AgrA/C. It is, therefore, unlikely that AgrD itself is the SIRL-1-activating molecule. Instead, the *agr*-encoded QS system components of *S. aureus* probably regulate the secretion of a SIRL-1 ligand. To test this hypothesis, we stimulated the hSIRL-1-CD3 $\zeta$  reporter cells with supernatants of NTML mutants in regulatory proteins that are under control of the *agr* system. These included mutants in the pentose phosphate pathway-responsive regulator *rpiR*, repressor of toxins *rot*,

endoribonuclease III *rnc*, and in two main staphylococcal protein secretion pathways—twin-arginine translocation system *tat/tatC* and the secretion system *secA/secY*—which are responsible for the transmembrane transport of most *S. aureus* secreted proteins. Supernatants from all these mutants induced GFP expression in hSIRL-1-CD3 $\zeta$  reporter cells, in contrast to the supernatants of *sarA*, *agrA*, *agrB*, and *agrC* NTML Tn-insertion mutants, which only induced minimal GFP expression (Figure 2B). Our data show that the SIRL-1 ligand secreted by *S. aureus* is directly regulated by the *agr* system and not through an interconnected regulatory system downstream of the *agr* system. Furthermore, it is not secreted via the major staphylococcal secretion systems Tat or Sec.

### 3.3 | Staphylococcal $\alpha$ -type phenol-soluble modulins (PSMs) activate SIRL-1

The staphylococcal QS system also controls the expression of PSMs, a family of peptides with distinct structural and functional characteristics, almost universally expressed by staphylococci. PSMs are amphipathic  $\alpha$ -helical peptides, that is, polar amino acids partition on one side of the helix and hydrophobic ones on the other.<sup>33</sup> Many PSMs are cytotoxic to human cells.<sup>33,46</sup> PSMs are typically formylated on the N'-terminal methionine and can activate the chemotactic FPR2 on immune cells.<sup>52</sup> In *S. aureus*, the shorter  $\alpha$ -type PSMs (20 to 26 amino acids) comprise PSM $\alpha$ 1-4 and  $\delta$ -toxin (*hld*), while the longer  $\beta$ -type PSMs comprise PSM $\beta$ 1-2 (44 amino acids). The expression of *psm* genes is strictly controlled by the direct binding of AgrA to the *psm* promoter region.<sup>46</sup> We tested overnight supernatants of the following independently generated deletion mutants: a quadruple *agrABCD* mutant lacking all four QS genes ( $\Delta$ *agr*),<sup>33</sup> a triple deletion mutant in PSM $\alpha$ 1-4, PSM $\beta$ 1-2, and  $\delta$ -toxin *hld* ( $\Delta$ PSM),<sup>34</sup> and single deletion mutants in PSM $\alpha$ 1-4 ( $\Delta$ PSM $\alpha$ ), PSM $\beta$ 1-2 ( $\Delta$ PSM $\beta$ ), or  $\delta$ -toxin ( $\Delta$ *hld*). To exclude strain-specific effects, we used mutants in two different genetic backgrounds, *S. aureus* strains LAC and MW2.  $\Delta$ *agr*,  $\Delta$ PSM, and  $\Delta$ PSM $\alpha$ 1-4 in both genetic backgrounds showed significantly decreased SIRL-1 activation in the reporter cell line, while  $\Delta$ PSM $\beta$ 1-2 and  $\Delta$ *hld* have no or very little (*hld*) effect on GFP expression, showing that PSM $\alpha$ 1-4 are possibly the SIRL-1 ligands (Figure 2C,E).

To confirm that genes encoding PSM $\alpha$ 1-4 confer SIRL-1-activating properties to *S. aureus* supernatants and exclude possible unwanted *in cis* effects of gene deletions, we performed a gene complementation study. Tetracycline resistance-bearing pTX $\Delta$ 16 plasmids encoding PSM $\alpha$ 1-4 (p-PSM $\alpha$ ), PSM $\beta$ 1-2 (p-PSM $\beta$ ), or  $\delta$ -toxin (p-*hld*) under control of constitutively active staphylococcal xylose promoter were introduced into the  $\Delta$ PSM strain. Empty pTX $\Delta$ 16 plasmid

backbone was introduced into wt and  $\Delta$ PSM strains as a control. We performed the plasmid complementation in *S. aureus* LAC (Figure 2D) and *S. aureus* MW2 (Figure 2F) genetic backgrounds. Reintroduction of genes encoding PSM $\alpha$ 1-4, but not PSM $\beta$ 1-2, into  $\Delta$ PSM mutants restored SIRL-1 reporter cell line activation to the levels induced by supernatants of wt strains. In contrast to our results with the *hld* deletion strains (Figure 2C,E), reintroduction of the gene encoding the  $\delta$ -toxin (p-*hld*) restored the SIRL-1-activating phenotype exhibited by the wt strain (Figure 2D,F). Notably, in *S. aureus* LAC, p-*hld* complementation resulted in lower numbers of GFP-positive SIRL-1 reporter cells compared to the wt strain. In *S. aureus* MW2, this difference was not significant, which we attribute to slight variability in data. A possible explanation for the observed restoration of SIRL-1 activation in the p-*hld* complemented strains while the *hld* deletions showed no effect on SIRL-1 activation is that in overnight supernatants of wt strains, the amounts of PSM $\alpha$ 1-4 may be higher than the amounts of  $\delta$ -toxin and may compensate for the effect of *hld* deletion. Furthermore, plasmid-encoded PSM genes are not controlled by their native promoter, but instead by a constitutively active xylose promoter. Additionally, the copy number of genes encoding PSMs on the plasmid is higher than on the chromosome. Both factors may result in higher supernatant concentrations of PSMs when expressed from the plasmid than when expressed from the chromosome. The empty vector backbone introduction into either wt or  $\Delta$ PSM backgrounds did not have any noticeable effect on GFP expression (Figure 2D,F).

To verify that no other bacterial co-factors were required for SIRL-1 activation, we determined whether synthetic  $\alpha$ -type PSMs activated the hSIRL-1-CD3 $\zeta$  reporter cell line. Naturally produced PSMs are predominantly N' terminally formylated. We stimulated reporter cells with plate-coated *S. aureus* N'-formyl-PSM $\alpha$ 3, N'-formyl-PSM $\beta$ 1, N'-formyl- $\delta$ -toxin, and non-formylated PSM $\alpha$ 3. The hSIRL-1-CD3 $\zeta$  reporter cell line was selectively activated by N'-formyl-PSM $\alpha$ 3, non-formylated PSM $\alpha$ 3, and N'-formyl  $\delta$ -toxin, but not N'-formyl-PSM $\beta$ 1, which is in line with our previous observations using bacterial gene knockouts (Figure 2C,E). The formylation status of PSM $\alpha$ 3 did not affect SIRL-1 activation. Notably, the observed SIRL-1-activating effect was concentration dependent (Figure 3A) and receptor specific, since wt and hLAIR-1-CD3 $\zeta$  reporter cell lines did not respond to any of the synthetic peptides (Figure 3B).

### 3.4 | Human antimicrobial peptide cathelicidin LL-37 activates SIRL-1

Cathelicidin LL-37 is a human host defense peptide that shows biochemical, structural, and functional similarities



to  $\alpha$ -type PSMs.<sup>56,57</sup> It is a 37 AA long amphipathic  $\alpha$ -helical peptide constitutively expressed by epithelial cells at barrier sites, such as the skin, and acts as a first defense against invading microbes.<sup>19</sup> Additionally, activated immune cells secrete it in high amounts to promote the inflammatory process.<sup>17,58-62</sup> LL-37 is produced by cleavage of its precursor protein hCAP18 by kallikrein in keratinocytes<sup>63</sup> and proteinase 3 in neutrophils.<sup>64</sup> It interacts with the membranes of bacteria and eukaryotic cells, impairing membrane integrity through pore formation, resulting in cytolysis.<sup>65,66</sup> In sub-cytolytic concentrations, LL-37 also regulates the immune system through binding to FPR2,<sup>67</sup> promoting immune cell activation to clear pathogens. We stimulated the hSIRL-1-CD3 $\zeta$  reporter cells with increasing concentrations of plate-coated LL-37 and observed that this  $\alpha$ -helical peptide activated the hSIRL-1-CD3 $\zeta$ , but not wt or hLAIR-1-CD3 $\zeta$ , reporter cells in a concentration-dependent manner (Figure 3C,D). This observation identifies a new endogenous candidate ligand for SIRL-1.

### 3.5 | SIRL-1 activation by PSMs and LL-37 is blocked by specific antibodies

To further demonstrate that the observed GFP signal is SIRL-1 specific, we pre-incubated the hSIRL-1-CD3 $\zeta$  reporter cells with two different anti-SIRL-1 antibodies (clones 1A5 and 3D3) or with the anti-LAIR-1 antibody (clone 8A8) before incubation on plate-coated PSM $\alpha$ 3, LL-37, and anti-CD3 antibody as control (Figure 3E-H). Pre-incubation of hSIRL-1-CD3 $\zeta$  reporter cells with anti-LAIR-1 or any of the anti-SIRL-1 antibodies did not affect the reporter cell activation by plate-coated anti-CD3 (Figure 3E). As an additional control, hLAIR-1-CD3 $\zeta$  reporter cells were pre-incubated with anti-LAIR-1 and both anti-SIRL-1 antibodies and subsequently stimulated with plate-coated collagen I. While anti-LAIR-1 blocked collagen I-induced LAIR-1 activation, none of the anti-SIRL-1 antibodies did so (Figure 3F). Both anti-SIRL-1 antibodies blocked the interaction between PSM $\alpha$ 3 or LL-37 and SIRL-1 in a concentration-dependent manner (Figure 3G,H). Thus, we have further confirmed that PSM $\alpha$ 3- and LL-37-induced GFP expression is specific for SIRL-1 and requires the SIRL-1 ectodomain.

To further investigate whether PSMs and LL-37 directly activate SIRL-1, we sought to measure reporter cell activation in a transcription-independent manner. We visualized and quantified the translocation of NFAT from the cytoplasm to the nucleus 30 min after incubation of hSIRL-1-CD3 $\zeta$  reporter cells with PBS, PMA-ionomycin, anti-CD3, anti-SIRL-1, anti-LAIR-1, PSM $\alpha$ 3, or cathelicidin LL-37 (Figure 3I shows visualization, and Figure 3J shows quantification). We observed NFAT translocation

from the cytoplasm into the nucleus after incubation with PMA-ionomycin, anti-CD3, and anti-SIRL-1, but not PBS or anti-LAIR-1, showing specificity (Figure 3I). Incubation with both PSM $\alpha$ 3 and cathelicidin LL-37 resulted in a substantial increase in nuclear NFAT (Figure 3J). These data strongly suggest that both *S. aureus* PSM $\alpha$ 3 and human cathelicidin LL-37 directly activate SIRL-1.

### 3.6 | SIRL-1 is broadly activated by staphylococcal PSMs

Virtually, all staphylococcal species express PSMs. At least 12 different PSMs and similar peptides are identified in *S. aureus*: PSM $\alpha$ 1-4, PSM $\beta$ 1-2,  $\delta$ -toxin, and its allelic variant G10S.<sup>33,43</sup> Furthermore, specific sub-types of methicillin-resistant *S. aureus* strains also possess PSM-Mec.<sup>44</sup> Additionally, three N'-terminal fragments of the QS protein AgrD of *S. aureus*—N-AgrD F20, N-AgrD F24, and N-AgrD D20—have been identified<sup>45</sup> with properties remarkably similar to other PSMs. In *S. epidermidis*, PSM $\beta$ 1-3, PSM $\alpha$ , PSM $\gamma$ / $\delta$ -toxin, PSM $\delta$ , and PSM $\epsilon$  were identified.<sup>46,47</sup> Furthermore, PSM $\beta$ 1-3 and PSM $\alpha$  in *S. haemolyticus*,<sup>48</sup> homologs of *S. epidermidis* PSM $\epsilon$  in *S. lugdunensis*, *S. pseudintermedius*, and *S. warneri*,<sup>49</sup> and the OrfX peptide in *S. lugdunensis*<sup>50</sup> are described. We synthesized these PSMs and stimulated the reporter cell lines with them (Figure 4A-C). All shorter PSM $\alpha$ -type peptides of *S. aureus*, except for PSM-Mec and the N'-terminal fragments of AgrD, strongly activated the hSIRL-1-CD3 $\zeta$ , but not wt or hLAIR-1-CD3 $\zeta$ , reporter cell line (Figure 4A). The longer PSM $\beta$ -type peptides did not induce significant GFP expression in hSIRL-1-CD3 $\zeta$  reporter cells (Figure 4A). Similarly, PSM $\alpha$ -type peptides of *S. epidermidis* and other staphylococci activated the hSIRL-1-CD3 $\zeta$ , but not wt or hLAIR-1-CD3 $\zeta$ , reporter cell line, while PSM $\beta$ -type peptides did not (Figure 4B,C). Therefore, we conclude that short, PSM $\alpha$ -like PSMs across the genus *Staphylococcus* activate SIRL-1.

### 3.7 | SIRL-1 recognizes amphipathic $\alpha$ -helical peptides

Among staphylococcal PSMs, sequence identity is low. The pairwise sequence identities between SIRL-1-activating *S. aureus* PSM $\alpha$ 3 and other SIRL-1-activating PSMs shown in Figure 4 range from 16% for *S. lugdunensis* OrfX to 41% for *S. aureus* PSM $\alpha$ 2, and the average pairwise sequence identity is only 24%. On the other hand, general structural properties are much more conserved among PSMs. In these peptides, the alternating arrangement of charged and hydrophobic amino acids from the N' to the C' terminus



results in their partitioning to the opposite sides of the  $\alpha$ -helix, giving rise to amphipathicity. Furthermore, an overall positive charge is seen in all SIRL-1-activating PSMs (except for *S. epidermidis* PSM $\alpha$ , which has a zero net charge but is still amphipathic). The same structural features are also recognized in the human cathelicidin LL-37, while its sequence identity to PSMs is low. To explore the structure–function relationship in SIRL-1-activating PSMs, we investigated how PSM-mediated SIRL-1 activation is affected by structural changes in PSMs such as change in chirality or C'–N' sequence reversal. We stimulated the hSIRL-1-CD3 $\zeta$  reporter cell line with the all-D isomer of *S. aureus* PSM $\alpha$ 3 or with C'–N' PSM $\alpha$ 3 and observed that these peptides activated SIRL-1 in the GFP reporter assay equally potently as the wt PSM $\alpha$ 3 (Figure 5A,B). This observation supports the idea that SIRL-1 recognizes a general molecular feature of staphylococcal PSMs instead of a particular amino acid sequence.

To further explore the structural characteristics of SIRL-1-activating peptides, we designed a series of PSM- and LL-37-inspired peptides with differing properties and tested these in wt, hLAIR-1-CD3 $\zeta$ , and hSIRL-1-CD3 $\zeta$  reporter cells (Figure 5C, Table 3). We varied the amino acid composition and their positioning in the  $\alpha$ -helix to vary: (1) overall/net charge of the helix; (2) partitioning of the charged and hydrophobic residues along the helix; and (3) overall hydrophobicity. We chose amino acids with the highest propensities to form  $\alpha$ -helices<sup>38</sup>: lysine to incorporate a positive charge, glutamic acid to incorporate a negative charge, glutamine as a polar uncharged amino acid, and leucine as a hydrophobic amino acid, and performed secondary structure prediction for all designed peptides. Most peptides were strongly predicted to have  $\alpha$ -helical secondary structure, except for peptides no. 2, 8, and 10–12, for which the  $\alpha$ -helical secondary structure prediction was less reliable. The secondary structure of peptide no. 6 could not be confidently predicted. To illustrate the peptides' amphipathicity, we plotted them as helical wheels (Figure 5C, peptide no. 1 is an example of an amphipathic peptide). Using this panel of rationally designed artificial peptides, we observed that all peptides with a predicted  $\alpha$ -helical secondary structure and amphipathic arrangement of hydrophobic residues activated SIRL-1 (Figure 5C). Notably, scrambling the positions of amino acids to disturb their separation to the polar and hydrophobic faces, and consequently, entirely disrupt the amphipathic character, while keeping the amino acid content unchanged, abrogated SIRL-1 activation (Figure 5C, peptide pairs 1-2, 3-4, and 7-8), except in the peptide pairs 5-6 (Figure 5C). The specific composition of the helix's polar face had little effect on SIRL-1-activating properties of the peptides (Figure 5C, peptides 13-28).

### 3.8 | Some artificial SIRL-1-activating peptides are non-toxic and do not activate FPR2

Most PSMs are highly cytotoxic and act pro-inflammatory by activating the chemotactic receptor FPR2 on immune cells.<sup>52</sup> We tested if the cytotoxic and FPR2-activating properties of our panel of designed peptides could be segregated from the SIRL-1-engaging property. We first assessed the cytotoxicity of all designed peptides by measuring LDH release from hSIRL-1-CD3 $\zeta$  reporter cells upon treatment with 10  $\mu$ M peptides. All derivatives of *S. aureus* PSM $\alpha$ 3 (PSM $\alpha$ 3, N'-formyl-PSM $\alpha$ 3, all-D-PSM $\alpha$ , and C'–N' PSM $\alpha$ 3) exhibited cytotoxicity (Figure 5D). In contrast, designed peptides 1-4, 7-12, and 18-22 were not cytotoxic at the same concentration (Figure 5D). We next screened a selection of non-toxic peptides for FPR2 activation by measuring Ca<sup>2+</sup> mobilization in the HL-60 cell line overexpressing FPR2. *S. aureus* PSM $\alpha$ 3 and its naturally occurring N'-formylated variant potently activated FPR2 (a representative transient Ca<sup>2+</sup> signal induced by PSM $\alpha$ 3 is shown in Figure 5E), and Ca<sup>2+</sup> signaling was entirely inhibited when cells were pre-incubated with the FPR2 inhibitory peptide WRW4 (Figure 5E,F). The C'–N' PSM $\alpha$ 3 and all-D-PSM $\alpha$ 3 did not activate FPR2, in line with previously published data.<sup>52</sup> None of the tested artificial SIRL-1-activating peptides activated FPR2 (Figure 5E,F). Therefore, cytotoxicity, FPR2 activation, and SIRL-1 engagement have different structural requirements. We here identified peptides 1, 3, and 18-22 as non-cytotoxic and non-FPR2-activating SIRL-1-specific agonists.

## 4 | DISCUSSION

Here, we demonstrate that secreted staphylococcal  $\alpha$ -helical peptides, PSMs,<sup>46,49</sup> activate the human inhibitory receptor SIRL-1. Our data show that in *S. aureus*, PSMs are the primary SIRL-1-activating compound, as PSM-deficient mutant strains have considerably decreased SIRL-1-activating properties. Nevertheless, PSM-deficient mutants still weakly engage SIRL-1, hinting at possible additional SIRL-1-activating factors secreted by staphylococci. For instance, these could be additional not yet characterized PSMs or similar molecules. We show that synthetic PSMs from other staphylococcal species also activate SIRL-1, demonstrating that SIRL-1 broadly recognizes staphylococcal PSMs. We further demonstrate that SIRL-1 is activated by the human peptide cathelicidin LL-37, which has structural and functional similarities to staphylococcal PSMs.<sup>19</sup> Taken together, we have identified a new group of bacterial and endogenous SIRL-1 ligands—the staphylococcal PSMs and the human cathelicidin LL-37.

PSMs are vital determinants of staphylococcal virulence: they are cytotoxic to different human cell types<sup>33</sup> and engage the chemotactic receptor FPR2 on human neutrophils.<sup>52</sup> They can be secreted in high amounts; it has been shown that as much as 60% of total secreted proteins in wt *S. aureus* USA300 are PSMs.<sup>49</sup> However, PSMs are not only virulence factors but also perform multiple other functions. They promote the spreading of bacterial cells on the epithelial surface<sup>49,68</sup> and facilitate the formation and structuring of biofilms.<sup>66,67</sup> PSMs also act as bacteriocins, cytotoxic bacterial products active against other bacterial species,<sup>34</sup> helping to maintain staphylococci in their habitat and protecting them and their host from other invading bacterial species. Furthermore, PSMs have immunomodulatory and tolerance-inducing properties. For example, they modulate human dendritic cells to direct the development of regulatory T cells, leading to tolerogenic immune responses.<sup>70,71</sup> All these features identify PSMs not only as virulence factors but also as facilitators of a mutually beneficial relationship between staphylococci and their host.

The human antimicrobial peptide cathelicidin LL-37 structurally and functionally resembles the staphylococcal PSMs. It is an amphipathic  $\alpha$ -helical peptide with cytotoxic and, through binding to FPR2, immunostimulatory properties.<sup>65-67</sup> However, it also possesses a plethora of immunomodulatory functions; it decreases the production of pro-inflammatory and stimulates the production of anti-inflammatory cytokines in numerous cell types. For example, LL-37 decreases pro-inflammatory cytokine production in epithelial cells pre-exposed to the bacterial TLR5 agonist flagellin,<sup>72</sup> decreases TNF and nitric oxide production in macrophage cell lines stimulated with LPS, LTA, or lipoarabinomannan PAMPs,<sup>73</sup> and dampens the expression of IL-6, IL-8, and CXCL10 induced by LPS in human gingival fibroblasts.<sup>74</sup> Future studies are needed to investigate the possibility that some of these modulatory functions are mediated by SIRL-1.

Recognition of PSMs and LL-37 by SIRL-1 does not require specific amino acid residues, which is evident from PSMs and LL-37 sharing little sequence identity. Instead, SIRL-1 may be activated by the general molecular features of these molecules. Based on the naturally occurring staphylococcal PSMs and the structurally and functionally similar human cathelicidin LL-37 that activate SIRL-1, we conclude that  $\alpha$ -helical peptides with an amphipathic arrangement of hydrophobicity engage SIRL-1. Furthermore, structural rearrangements of PSM $\alpha$ 3, such as in the all-D-PSM $\alpha$ 3 isomer and the C'-N' reversed sequence PSM $\alpha$ 3, in which  $\alpha$ -helical secondary structure and amphipathic arrangement of hydrophobic amino acid residues are preserved, still activate SIRL-1. Similar to our observation that both L- and D-PSM $\alpha$ 3 potently

activate SIRL-1, both L-LL-37 and D-LL-37 equally induce IL-8 production in human keratinocytes, which could be blocked by surface receptor-specific inhibitors.<sup>75</sup> It has been suggested that the hydrophobic environment of the cell membrane might allow for specific peptide-peptide or peptide-protein interactions irrespectively of the peptide's chirality or helix sense.<sup>76</sup> We could not demonstrate a direct interaction between PSMs or LL-37 and SIRL-1 in a purified system using recombinant proteins. This may indicate that a membrane component, which is absent in purified systems, is required for SIRL-1-PSM or SIRL-1-LL-37 complex formation. Our attempts to detect interaction may have additionally been hampered by the potent and irreversible tendency of these peptides to stack into amyloid-like fibrils.<sup>56,57</sup>

Based on the structural features of staphylococcal PSMs and the human LL-37, we rationally designed a series of peptides with predicted  $\alpha$ -helical secondary structure and varying amphipathic character, charge, and charge distribution. We observed that the amphipathic character of these peptides is required for SIRL-1 activation, regardless of the detailed variations in their structure. Although we did not experimentally determine the secondary structure of these peptides, the predicted secondary structure, together with the peptides' SIRL-1-activating properties, support our idea that  $\alpha$ -helical peptides with an amphipathic arrangement of hydrophobicity engage SIRL-1. Notably, scrambling the amino acids' positions to disturb their separation to the polar and hydrophobic faces, and consequently entirely disrupting the amphipathic character of the designed peptides while keeping their amino acid content unchanged, abrogated SIRL-1 engagement in all but one peptide pair (Figure 5C, peptide pairs 5-6). However, SIRL-1 engagement by both these peptides is much less prominent than with other peptides. Without further characterizing these peptides, we cannot adequately explain why peptide 6 still weakly engages SIRL-1. Finally, the charge distribution and overall charge of the artificial peptides did not have a notable effect on SIRL-1 activation.

General structural features of staphylococcal PSMs are formylation of the N'-terminal methionine,  $\alpha$ -helical secondary structure, and amphipathic arrangement of amino acid residues. Functionally, PSMs are cytotoxic and FPR2 activating, and as we show here, they also engage SIRL-1. Using the series of designed peptides, we were able to decouple the cytotoxic and pro-inflammatory properties of these peptides from their SIRL-1-engaging function. As expected, all derivatives of PSM $\alpha$ 3 (PSM $\alpha$ 3, N'-formyl-PSM $\alpha$ 3, all-D-PSM $\alpha$ , and C'-N' PSM $\alpha$ 3) exhibited cytotoxicity, while peptides with a lower net charge showed decreased or no cytotoxicity. This is in line with the fact that antimicrobial or cytotoxic peptides are commonly amphipathic and positively charged.<sup>77</sup> With regard to

FPR2 activation, we confirm that C'-N' reversed and all-D-PSM $\alpha$ 3 completely lost the FPR2-activating property, in line with previously published data.<sup>52</sup> Thus, we have obtained a group of LL-37- and PSM-inspired SIRL-1-engaging peptides without FPR2-activating and cytotoxic properties, demonstrating that different structural features of PSMs and LL-37 mediate FPR2 activation, SIRL-1 activation, and cytotoxicity. Others previously showed that different epitopes of the LL-37 peptide mediate different functions and that segregation of the peptide's functions is possible.<sup>75</sup> The ability to segregate the versatile properties of LL-37 and the PSMs is interesting from a therapeutic perspective, since inhibitory receptors are attractive targets for immunotherapy.<sup>78</sup>

Microbes rapidly evolve and quickly change their molecular makeup. To achieve reliable recognition of microbes, the immune system employs PRRs, which recognize general structural patterns to ensure robust target recognition that is not perturbed by minor changes in the ligands. Many known PRRs recognize more than one structural pattern. For example, the receptors RAGE, TLR4, and TLR2 all recognize different patterns and bind diverse ligands.<sup>79,80</sup> SIRL-1 may employ a similar strategy to recognize its ligands. We previously showed that SIRL-1 is activated by the human S100 proteins.<sup>11</sup> Here, we identify staphylococcal  $\alpha$ -type PSMs and human cathelicidin LL-37 as an additional class of SIRL-1 ligands. Both cathelicidin LL-37 and the S100 family of proteins are DAMPs and are released from damaged cells or activated immune cells to promote inflammatory processes. We have previously suggested that inhibitory receptors provide negative feedback on immune cell activation to prevent immunopathology.<sup>4</sup> In this regard, the recognition of DAMPs such as LL-37 by SIRL-1 may enable prompt cessation of inflammatory processes and limit immunopathology. The interaction between SIRL-1 and its newly described exogenous ligands, staphylococcal PSMs, may serve a similar purpose. It may be in place to favor the commensal lifestyle of PSM-producing staphylococci over their potential to trigger host-damaging immune responses.

A genetic polymorphism causing reduced SIRL-1 expression levels on monocytes is associated with atopic dermatitis, a skin disease characterized by extensive inflammation and almost universal presence of *S. aureus* in atopic dermatitis skin lesions.<sup>7,22</sup> On the other hand, atopic dermatitis is correlated with significantly lower or even insufficient LL-37 expression, especially after skin injury,<sup>81-83</sup> while in other inflammatory skin diseases, such as rosacea and psoriasis,<sup>84,85</sup> LL-37 expression is commonly increased. Together, this may suggest that the malfunction or absence of the PSM/LL-37-SIRL-1 regulatory axis, which would deliver inhibitory signals to immune cells, contributes to the development of inflammatory diseases like atopic dermatitis.

To conclude, we have demonstrated that SIRL-1 is activated by  $\alpha$ -helical peptides with an amphipathic arrangement of hydrophobicity, namely the human cathelicidin LL-37 and the staphylococcal PSMs. We designed SIRL-1-specific activating peptides without cytotoxic and chemotactic properties. This will allow us to unravel the biology of SIRL-1 further and will facilitate the development of SIRL-1 agonists for possible therapeutic intervention in autoimmune and inflammatory diseases.

## ACKNOWLEDGMENTS

We want to thank Bas Surewaard for providing the following plasmids: pTX $\Delta$ 16, pTX $\Delta$ 16-PSM $\alpha$ , pTX $\Delta$ 16-PSM $\beta$ , and pTX $\Delta$ 16-*hld*. This work was supported by a Vici grant from the Netherlands Organization for Scientific Research awarded to LM (NWO, grant no. 91815608).

## DISCLOSURES

The authors state explicitly that there are no conflicts of interest to declare in connection with this article.

## AUTHOR CONTRIBUTIONS

MR, NMv.S., and LM designed the study. MR, HJv.R., M.v.d.L., and GHAW performed the experiments and analyzed the data. CTO synthesized the peptides. MR wrote the manuscript. All authors except HO contributed to the reviewing and editing of the final manuscript. ML, HO, NMv.S., and LM supervised the study. LM acquired funding for the study.

## ORCID

Matevž Rumpret  <https://orcid.org/0000-0002-8631-8049>

Helen J. von Richthofen  <https://orcid.org/0000-0002-2062-5986>

Maarten van der Linden  <https://orcid.org/0000-0001-8597-4151>

Cami Talavera Ormeño  <https://orcid.org/0000-0001-5502-2985>

Jos A. G. van Strijp  <https://orcid.org/0000-0001-6253-0830>

Meytal Landau  <https://orcid.org/0000-0002-1743-3430>

Nina M. van Sorge  <https://orcid.org/0000-0002-2695-5863>

Linde Meyaard  <https://orcid.org/0000-0003-0707-4793>

## REFERENCES

1. Akira S, Uematsu S, Takeuchi O. Pathogen recognition and innate immunity. *Cell*. 2006;124:783-801.
2. Yang D, Yang Z, Oppenheim JJ. Alarmins and immunity. *Immunol Rev*. 2017;280:41-56.
3. Bianchi ME. DAMPs, PAMPs and alarmins: all we need to know about danger. *J Leukoc Biol*. 2007;81:1-5.
4. Rumpret M, Drylewicz J, Ackermans LJE, Borghans JAM, Medzhitov R, Meyaard L. Functional categories of immune inhibitory receptors. *Nat Rev Immunol*. 2020;20:771-780.



5. Steevels TA, Lebbink RJ, Westerlaken GH, Coffey PJ, Meyaard L. Signal inhibitory receptor on leukocytes-1 is a novel functional inhibitory immune receptor expressed on human phagocytes. *J Immunol.* 2010;184:4741-4748.
6. von Richthofen HJ, Gollnast D, van Capel TMM, et al. Signal inhibitory receptor on leukocytes-1 is highly expressed on lung monocytes, but absent on mononuclear phagocytes in skin and colon. *Cell Immunol.* 2020;357:104199.
7. Kumar D, Puan KJ, Andiappan AK, et al. A functional SNP associated with atopic dermatitis controls cell type-specific methylation of the VSTM1 gene locus. *Genome Med.* 2017;9:18.
8. Steevels TA, van Avondt K, Westerlaken GH, et al. Signal inhibitory receptor on leukocytes-1 (SIRL-1) negatively regulates the oxidative burst in human phagocytes. *Eur J Immunol.* 2013;43:1297-1308.
9. Van Avondt K, Fritsch-Stork R, Derksen RH, Meyaard L. Ligation of signal inhibitory receptor on leukocytes-1 suppresses the release of neutrophil extracellular traps in systemic lupus erythematosus. *PLoS One.* 2013;8:e78459.
10. Van Avondt K, van der Linden M, Naccache PH, Egan DA, Meyaard L. Signal inhibitory receptor on leukocytes-1 limits the formation of neutrophil extracellular traps, but preserves intracellular bacterial killing. *J Immunol.* 2016;196:3686-3694.
11. Rumpert M, von Richthofen HJ, van der Linden M, et al. Recognition of S100 proteins by Signal Inhibitory Receptor on Leukocytes-1 negatively regulates human neutrophils. *Eur J Immunol.* 2021;51:2210-2217.
12. Besteman SB, Callaghan A, Hennis MP, Westerlaken GHA, Meyaard L, Bont LL. Signal inhibitory receptor on leukocytes (SIRL)-1 and leukocyte-associated immunoglobulin-like receptor (LAIR)-1 regulate neutrophil function in infants. *Clin Immunol.* 2020;211:108324.
13. Christensen GJ, Bruggemann H. Bacterial skin commensals and their role as host guardians. *Benef Microbes.* 2014;5:201-215.
14. Cogen AL, Nizet V, Gallo RL. Skin microbiota: a source of disease or defence? *Br J Dermatol.* 2008;158:442-455.
15. Glaser R, Harder J, Lange H, Bartels J, Christophers E, Schroder JM. Antimicrobial psoriasis (S100A7) protects human skin from *Escherichia coli* infection. *Nat Immunol.* 2005;6:57-64.
16. Schroder JM, Harder J. Human beta-defensin-2. *Int J Biochem Cell Biol.* 1999;31:645-651.
17. Lai Y, Gallo RL. AMPed up immunity: how antimicrobial peptides have multiple roles in immune defense. *Trends Immunol.* 2009;30:131-141.
18. Schitteck B. The multiple facets of dermcidin in cell survival and host defense. *J Innate Immun.* 2012;4:349-360.
19. Vandamme D, Landuyt B, Luyten W, Schoofs L. A comprehensive summary of LL-37, the factotum human cathelicidin peptide. *Cell Immunol.* 2012;280:22-35.
20. Krismer B, Weidenmaier C, Zipperer A, Peschel A. The commensal lifestyle of *Staphylococcus aureus* and its interactions with the nasal microbiota. *Nat Rev Microbiol.* 2017;15:675-687.
21. Williams MR, Nakatsuji T, Gallo RL. *Staphylococcus aureus*: master manipulator of the skin. *Cell Host Microbe.* 2017;22:579-581.
22. Geoghegan JA, Irvine AD, Foster TJ. *Staphylococcus aureus* and atopic dermatitis: a complex and evolving relationship. *Trends Microbiol.* 2018;26:484-497.
23. Lowy FD. *Staphylococcus aureus* infections. *N Engl J Med.* 1998;339:520-532.
24. Edwards AM, Massey RC. How does *Staphylococcus aureus* escape the bloodstream? *Trends Microbiol.* 2011;19:184-190.
25. Becker K, Heilmann C, Peters G. Coagulase-negative staphylococci. *Clin Microbiol Rev.* 2014;27:870-926.
26. Brown MM, Horswill AR. *Staphylococcus epidermidis*—skin friend or foe? *PLoS Pathog.* 2020;16:e1009026.
27. Byrd AL, Belkaid Y, Segre JA. The human skin microbiome. *Nat Rev Microbiol.* 2018;16:143-155.
28. O'Riordan K, Lee JC. *Staphylococcus aureus* capsular polysaccharides. *Clin Microbiol Rev.* 2004;17:218-234.
29. Foster TJ. Immune evasion by staphylococci. *Nat Rev Microbiol.* 2005;3:948-958.
30. de Jong NWM, van Kessel KPM, van Strijp JAG. Immune evasion by *Staphylococcus aureus*. *Microbiol Spectr.* 2019;7.
31. Otto M, O'Mahoney DS, Guina T, Klebanoff SJ. Activity of *Staphylococcus epidermidis* phenol-soluble modulins expressed in *Staphylococcus carnosus*. *J Infect Dis.* 2004;190:748-755.
32. Van Avondt K, van Sorge NM, Meyaard L. Bacterial immune evasion through manipulation of host inhibitory immune signaling. *PLoS Pathog.* 2015;11:e1004644.
33. Wang R, Braughton KR, Kretschmer D, et al. Identification of novel cytolytic peptides as key virulence determinants for community-associated MRSA. *Nat Med.* 2007;13:1510-1514.
34. Joo HS, Cheung GY, Otto M. Antimicrobial activity of community-associated methicillin-resistant *Staphylococcus aureus* is caused by phenol-soluble modulins derivatives. *J Biol Chem.* 2011;286:8933-8940.
35. Periasamy S, Joo HS, Duong AC, et al. How *Staphylococcus aureus* biofilms develop their characteristic structure. *Proc Natl Acad Sci U S A.* 2012;109:1281-1286.
36. Dastgheyb SS, Villaruz AE, Le KY, et al. Role of phenol-soluble modulins in formation of *Staphylococcus aureus* biofilms in synovial fluid. *Infect Immun.* 2015;83:2966-2975.
37. Nakamura Y, Oscherwitz J, Cease KB, et al. *Staphylococcus delta-toxin* induces allergic skin disease by activating mast cells. *Nature.* 2013;503:397-401.
38. Nick Pace C, Martin SJ. A helix propensity scale based on experimental studies of peptides and proteins. *Biophys J.* 1998;75:422-427.
39. Sievers F, Wilm A, Dineen D, et al. Fast, scalable generation of high-quality protein multiple sequence alignments using Clustal Omega. *Mol Syst Biol.* 2011;7:539.
40. Drozdetskiy A, Cole C, Procter J, Barton GJ. JPred4: a protein secondary structure prediction server. *Nucleic Acids Res.* 2015;43:W389-W394.
41. Gautier R, Douquet D, Antonny B, Drin G. HELIQUEST: a web server to screen sequences with specific alpha-helical properties. *Bioinformatics.* 2008;24:2101-2102.
42. Larrick JW, Hirata M, Balint RF, Lee J, Zhong J, Wright SC. Human CAP18: a novel antimicrobial lipopolysaccharide-binding protein. *Infect Immun.* 1995;63:1291-1297.
43. Cheung GY, Yeh AJ, Kretschmer D, et al. Functional characteristics of the *Staphylococcus aureus* delta-toxin allelic variant G10S. *Sci Rep.* 2015;5:18023.
44. Qin L, McCausland JW, Cheung GY, Otto M. PSM-Mec—a virulence determinant that connects transcriptional regulation, virulence, and antibiotic resistance in Staphylococci. *Front Microbiol.* 2016;7:1293.

45. Schwartz K, Sekedat MD, Syed AK, et al. The AgrD N-terminal leader peptide of *Staphylococcus aureus* has cytolytic and amyloidogenic properties. *Infect Immun*. 2014;82:3837-3844.
46. Otto M. Phenol-soluble modulins. *Int J Med Microbiol*. 2014;304:164-169.
47. Wang R, Khan BA, Cheung GY, et al. *Staphylococcus epidermidis* surfactant peptides promote biofilm maturation and dissemination of biofilm-associated infection in mice. *J Clin Invest*. 2011;121:238-248.
48. Da F, Joo HS, Cheung GYC, et al. Phenol-soluble modulin toxins of *Staphylococcus haemolyticus*. *Front Cell Infect Microbiol*. 2017;7:206.
49. Cheung GY, Joo HS, Chatterjee SS, Otto M. Phenol-soluble modulins—critical determinants of staphylococcal virulence. *FEMS Microbiol Rev*. 2014;38:698-719.
50. Rautenberg M, Joo HS, Otto M, Peschel A. Neutrophil responses to staphylococcal pathogens and commensals via the formyl peptide receptor 2 relates to phenol-soluble modulin release and virulence. *FASEB J*. 2011;25:1254-1263.
51. Lebbink RJ, de Ruiter T, Adelmeijer J, et al. Collagens are functional, high affinity ligands for the inhibitory immune receptor LAIR-1. *J Exp Med*. 2006;203:1419-1425.
52. Kretschmer D, Gleske AK, Rautenberg M, et al. Human formyl peptide receptor 2 senses highly pathogenic *Staphylococcus aureus*. *Cell Host Microbe*. 2010;7:463-473.
53. Novick RP, Geisinger E. Quorum sensing in staphylococci. *Annu Rev Genet*. 2008;42:541-564.
54. Lyon GJ, Mayville P, Muir TW, Novick RP. Rational design of a global inhibitor of the virulence response in *Staphylococcus aureus*, based in part on localization of the site of inhibition to the receptor-histidine kinase, AgrC. *Proc Natl Acad Sci U S A*. 2000;97:13330-13335.
55. Cheung AL, Projan SJ. Cloning and sequencing of sarA of *Staphylococcus aureus*, a gene required for the expression of agr. *J Bacteriol*. 1994;176:4168-4172.
56. Tayeb-Fligelman E, Tabachnikov O, Moshe A, et al. The cytotoxic *Staphylococcus aureus* PSMalpha3 reveals a cross-alpha amyloid-like fibril. *Science*. 2017;355:831-833.
57. Engelberg Y, Landau M. The human LL-37(17–29) antimicrobial peptide reveals a functional supramolecular structure. *Nat Commun*. 2020;11:3894.
58. Malm J, Sorensen O, Persson T, et al. The human cationic antimicrobial protein (hCAP-18) is expressed in the epithelium of human epididymis, is present in seminal plasma at high concentrations, and is attached to spermatozoa. *Infect Immun*. 2000;68:4297-4302.
59. Frohm M, Agerberth B, Ahangari G, et al. The expression of the gene coding for the antibacterial peptide LL-37 is induced in human keratinocytes during inflammatory disorders. *J Biol Chem*. 1997;272:15258-15263.
60. Hase K, Eckmann L, Leopard JD, Varki N, Kagnoff MF. Cell differentiation is a key determinant of cathelicidin LL-37/human cationic antimicrobial protein 18 expression by human colon epithelium. *Infect Immun*. 2002;70:953-963.
61. Bals R, Wang X, Zasloff M, Wilson JM. The peptide antibiotic LL-37/hCAP-18 is expressed in epithelia of the human lung where it has broad antimicrobial activity at the airway surface. *Proc Natl Acad Sci U S A*. 1998;95:9541-9546.
62. Xhindoli D, Pacor S, Benincasa M, Scocchi M, Gennaro R, Tossi A. The human cathelicidin LL-37–A pore-forming antibacterial peptide and host-cell modulator. *Biochim Biophys Acta*. 2016;1858:546-566.
63. Morizane S, Yamasaki K, Kabigting FD, Gallo RL. Kallikrein expression and cathelicidin processing are independently controlled in keratinocytes by calcium, vitamin D(3), and retinoic acid. *J Invest Dermatol*. 2010;130:1297-1306.
64. Sorensen OE, Follin P, Johnsen AH, et al. Human cathelicidin, hCAP-18, is processed to the antimicrobial peptide LL-37 by extracellular cleavage with proteinase 3. *Blood*. 2001;97:3951-3959.
65. Oren Z, Lerman JC, Gudmundsson GH, Agerberth B, Shai Y. Structure and organization of the human antimicrobial peptide LL-37 in phospholipid membranes: relevance to the molecular basis for its non-cell-selective activity. *Biochem J*. 1999;341(Pt 3):501-513.
66. Thennarasu S, Tan A, Penumatchu R, Shelburne CE, Heyl DL, Ramamoorthy A. Antimicrobial and membrane disrupting activities of a peptide derived from the human cathelicidin antimicrobial peptide LL37. *Biophys J*. 2010;98:248-257.
67. Coffelt SB, Tomchuck SL, Zvezdaryk KJ, Danka ES, Scandurro AB. Leucine leucine-37 uses formyl peptide receptor-like 1 to activate signal transduction pathways, stimulate oncogenic gene expression, and enhance the invasiveness of ovarian cancer cells. *Mol Cancer Res*. 2009;7:907-915.
68. Tsompanidou E, Denham EL, Becher D, et al. Distinct roles of phenol-soluble modulins in spreading of *Staphylococcus aureus* on wet surfaces. *Appl Environ Microbiol*. 2013;79:886-895.
69. Schwartz K, Syed AK, Stephenson RE, Rickard AH, Boles BR. Functional amyloids composed of phenol soluble modulins stabilize *Staphylococcus aureus* biofilms. *PLoS Pathog*. 2012;8:e1002744.
70. Armbruster NS, Richardson JR, Schreiner J, Klenk J, Gunter M, Autenrieth SE. *Staphylococcus aureus* PSM peptides induce tolerogenic dendritic cells upon treatment with ligands of extracellular and intracellular TLRs. *Int J Med Microbiol*. 2016;306:666-674.
71. Richardson JR, Armbruster NS, Gunter M, Henes J, Autenrieth SE. *Staphylococcus aureus* PSM peptides modulate human monocyte-derived dendritic cells to prime regulatory T cells. *Front Immunol*. 2018;9:2603.
72. Pistolic J, Cosseau C, Li Y, et al. Host defence peptide LL-37 induces IL-6 expression in human bronchial epithelial cells by activation of the NF-kappaB signaling pathway. *J Innate Immun*. 2009;1:254-267.
73. Scott MG, Davidson DJ, Gold MR, Bowdish D, Hancock RE. The human antimicrobial peptide LL-37 is a multifunctional modulator of innate immune responses. *J Immunol*. 2002;169:3883-3891.
74. Into T, Inomata M, Shibata K, Murakami Y. Effect of the antimicrobial peptide LL-37 on Toll-like receptors 2-, 3- and 4-triggered expression of IL-6, IL-8 and CXCL10 in human gingival fibroblasts. *Cell Immunol*. 2010;264:104-109.
75. Braff MH, Hawkins MA, Di Nardo A, et al. Structure-function relationships among human cathelicidin peptides: dissociation of antimicrobial properties from host immunostimulatory activities. *J Immunol*. 2005;174:4271-4278.
76. Tomasinsig L, Pizzirani C, Skerlavaj B, et al. The human cathelicidin LL-37 modulates the activities of the P2X7 receptor in a structure-dependent manner. *J Biol Chem*. 2008;283:30471-30481.
77. Brogden KA. Antimicrobial peptides: pore formers or metabolic inhibitors in bacteria? *Nat Rev Microbiol*. 2005;3:238-250.



78. van der Vlist M, Kuball J, Radstake TR, Meyaard L. Immune checkpoints and rheumatic diseases: what can cancer immunotherapy teach us? *Nat Rev Rheumatol*. 2016;12:593-604.
79. Sims GP, Rowe DC, Rietdijk ST, Herbst R, Coyle AJ. HMGB1 and RAGE in inflammation and cancer. *Annu Rev Immunol*. 2010;28:367-388.
80. Erridge C. Endogenous ligands of TLR2 and TLR4: agonists or assistants? *J Leukoc Biol*. 2010;87:989-999.
81. Ong PY, Ohtake T, Brandt C, et al. Endogenous antimicrobial peptides and skin infections in atopic dermatitis. *N Engl J Med*. 2002;347:1151-1160.
82. Mallbris L, Carlen L, Wei T, et al. Injury downregulates the expression of the human cathelicidin protein hCAP18/LL-37 in atopic dermatitis. *Exp Dermatol*. 2010;19:442-449.
83. Kanda N, Hau CS, Tada Y, Sato S, Watanabe S. Decreased serum LL-37 and vitamin D3 levels in atopic dermatitis: relationship between IL-31 and oncostatin M. *Allergy*. 2012;67:804-812.
84. Yamasaki K, Di Nardo A, Bardan A, et al. Increased serine protease activity and cathelicidin promotes skin inflammation in rosacea. *Nat Med*. 2007;13:975-980.
85. Morizane S, Yamasaki K, Muhleisen B, et al. Cathelicidin antimicrobial peptide LL-37 in psoriasis enables keratinocyte reactivity against TLR9 ligands. *J Invest Dermatol*. 2012;132:135-143.

**How to cite this article:** Rumpret M, von Richthofen HJ, van der Linden M, et al. Signal inhibitory receptor on leukocytes-1 recognizes bacterial and endogenous amphipathic  $\alpha$ -helical peptides. *FASEB J*. 2021;35:e21875. <https://doi.org/10.1096/fj.202100812R>

## APPENDIX

**TABLE A1** NTML screening hits that were excluded from further analysis

NE number	% GFP-positive SIRT1-CD3 $\zeta$ cells	Gene	Gene product
NE169	4.1	<i>cap5P</i>	Capsular polysaccharide biosynthesis protein Cap5P
NE352	5.6	<i>rsgA</i>	Ribosome small subunit-dependent GTPase A
NE592	2.8	<i>atpA</i>	ATP synthase F1, alpha subunit
NE883	5.4	<i>xerC</i>	Tyrosine recombinase XerC
NE974	6.4	<i>mutS</i>	DNA mismatch repair protein MutS
NE1048	4.7	<i>pyrP</i>	Uracil permease
NE1205	6.4	<i>nrdG</i>	Anaerobic ribonucleotide reductase, small subunit
NE1262	4.1	—	Putative membrane protein (SAUSA300_1984)
NE1509	3.0	<i>mdlB</i>	ABC transporter, ATP-binding protein
NE1531	4.9	<i>pdxT</i>	Glutamine amidotransferase subunit PdxT
NE1656	4.4	<i>ribD</i>	Riboflavin biosynthesis protein
NE1713	4.9	<i>alr</i>	Alanine racemase
NE1829	2.7	<i>acoB</i>	2-oxoisovalerate dehydrogenase, E1 component, beta subunit
NE1895	6.4	<i>argR</i>	Arginine repressor
NE1896	2.3	<i>lpdA</i>	Dihydrolipoamide dehydrogenase
NE1908	3.4	<i>ccmA</i>	ABC transporter, ATP-binding protein